Liver

Laura A. Dawson, Oyedele Adeyi, Anne Horgan, and Chandan Guha

Contents

L. A. Dawson (✉)
Department of Radiation Oncology, Princess Margaret Hospital, University of Toronto, 610 University Avenue, Toronto, ON M5G 2M9, Canada
e-mail: laura.dawson@rmp.uhn.on.ca

O. Adeyi
Department of Pathology (Rm. 11E210), University of Toronto, Toronto General Hospital, 200 Elizabeth Street, Toronto, ON M5G 2C4, Canada

A. Horgan
Department of Medical Oncology, Waterford Regional Hospital, Waterford, Ireland

C. Guha
Department of Radiation Oncology, Montefiore Medical Center, Albert Einstein College of Medicine, 111 East 210 Street, Bronx, NY 10467, USA

Abstract

- The hepatic toxicity related to radiation therapy is classic radiation-induced liver disease (RILD) which presents within 3 months following radiation therapy with anicteric ascites and hepatosplenomegaly, characterized with central and sublobular hepatic vein occlusive lesions, with sparing of the periportal areas, larger hepatic veins, and hepatic arterial vasculature.
- No established standard exists.
- In 2 Gy per fraction, the mean liver doses estimated to be associated with a 5 % risk of classic RILD for primary and metastatic liver cancer are 28 and 32 Gy.
- Other non-classic RILD radiation hepatic toxicities include hepatitis and a general decline in liver function that may be precipitated by radiation therapy.
- TGF-β has been implicated in playing a role in the fibrogenesis leading up to RILD.
- Irradiation of rat liver in vivo induces upregulation of proinflammatory cytokines IL-1-beta, IL-6, and tumor necrosis factor alpha (Christiansen et al. in Radiology 242:189–197, 2007).

P. Rubin et al. (eds.), *ALERT – Adverse Late Effects of Cancer Treatment*, Medical Radiology. Radiation Oncology,
DOI: 10.1007/978-3-540-75863-1_15,

- Changes in CT and MRI contrast enhancement have been seen within regions of the liver (Herfarth et al. in Int J Radiat Oncol Biol Phys 57:444–451, 2003).
- Veno-occlusive disease (VOD) is a frequent, serious, and often life threatening complication of hematopoietic stem cell or bone marrow transplantation.
- Patterns of chemotherapy liver toxicity include: hepatitis, cholestasis, steatosis, fibrosis, and vascular lesions.
- Hepatic toxicity related to chemotherapy is usually idiosyncratic, unpredictable, and not dose-related.
- Direct hepatocellular injury from chemotherapy is less common and predictable.
- Baseline liver function tests and imaging, with serial re-evaluation, can aid in determining the cause of deteriorating liver function which may be related to underlying liver dysfunction, reactivation of a dormant virus, drug, or the cancer itself.

Abbreviations

APR	Acute phase reactant
AST	Aspartate transaminase
ALT	Alanine transaminase
ASGPR	Asialoglycoprotein receptor
BUdR	Bromodeoxyuridine
BMT	Bone marrow transplantation
CTCAE	Common terminology criteria for adverse events
CLIP	Cancer of the liver Italian program
CT	Computed tomographic
DVHs	Dose–volume histograms
RBCs	Erythrocytes
FUdR	Fluorodeoxyuridine
GIT	Gastrointestinal tract
GSH	Glutathione
HBV	Hepatitis B virus
HCC	Hepatocellular carcinoma
HSC	Hepatic stellate cell
ICG	Indocyanine Green
IVC	Inferior vena cava
IMRT	Intensity modulated radiation therapy
IORT	Intraoperative radiation therapy
NTCP	Normal tissue complication probability
RILD	Radiation-induced liver disease
RTOG	Radiation Therapy Oncology Group
RHV	Right hepatic vein
SECs	Sinusoidal endothelial cells
SOS	Sinusoidal obstructive syndrome
SMA	Smooth muscle actin
SPECT	Single-photon emission computerized tomography
SBRT	Stereotactic body radiotherapy
TACE	Transarterial chemo-embolization
TBI	Total body irradiation
TGF-β	Transforming growth factor-β
VOD	Veno-occlusive disease

1 Introduction

Irradiation of the liver is required in the treatment of many cancers, including those of the upper abdomen (e.g. hepatocellular carcinoma, cholangiocarcinoma, pancreatic carcinoma, gastric carcinoma), cancers near the upper abdomen (lower thoracic cancers, mesothelioma, retroperitoneal sarcoma) and following hematopoietic stem cell transplant and total body irradiation. The liver is a critically important organ that plays many vital roles. It aids in the digestive process with the production of bile, facilitating the metabolism of ingested nutrients, and the elimination of many waste products; it is involved in glycogen storage, decomposition of red blood cells, plasma protein synthesis, and detoxification. Injury to the liver can range from transient, clinically unimportant parenchymal damage that is only detected via serum measurements of enzymes leaked from damaged hepatocytes, or subclinical transient changes on imaging, to fatal hepatic insufficiency characterized by decreased production of proteins such as albumin and blood clotting factors, ascites, bleeding predilection, and encephalopathy.

The first type of radiation-associated liver toxicity described, termed classic radiation-induced liver disease (RILD) (Lawrence et al. 1995), presented as anicteric ascites, hepatomegaly, and elevated alkaline phosphatase following whole abdominal radiation therapy. Other liver toxicities seen following liver irradiation (termed 'non-classic RILD') include a general decline in liver function, elevation of liver enzymes, and reactivation of viral hepatitis. These toxicities are more common following irradiation of patients with an impaired liver functional reserve (for example, with cirrhosis). Veno-occlusive disease (VOD) can occur following stem cell transplant with or without total body irradiation. This differs in its presentation from classic RILD, in that elevated bilirubin is part of the diagnostic criteria (vs. little change in bilirubin in classic RILD). Both classic and nonclassic RILD can lead to liver failure and death, and avoidance of any liver toxicity following irradiation is always desirable.

The whole liver tolerance to irradiation is low. The partial volume tolerance of the liver is better understood for classic RILD than nonclassic RILD. For classic RILD, mean dose to the liver is correlated with RILD risk. A variety of dose/volume parameters can be used to provide clinical guidelines (Sect. 5). The toxicity models are highly

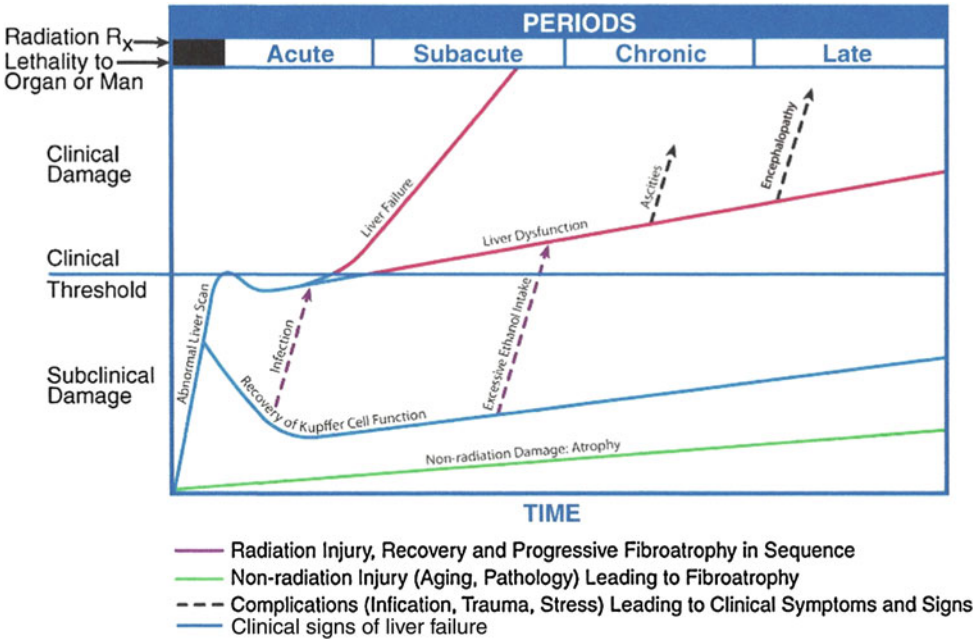

Fig. 1 The time course of liver symptoms in patients treated with radiation therapy (with permission from Rubin and Casarett 1968)

dependent on the patient population, presence of underlying liver disease (hepatitis B or C infection, or cirrhosis), radiation dose fractionation, and the toxicity endpoint investigated.

The pathophysiology of classic and non-classic RILD is becoming better understood (Sect. 3), but there is still much to learn in order to develop interventions that may mitigate the development of liver toxicity (Sect. 8). In this chapter, we will review radiation liver toxicity and provide dose/volume recommendations for the clinician.

Figure 1 summarizes timeline of our understanding of radiation liver toxicity.

2 Anatomy and Histology

2.1 Anatomy

2.1.1 Gross Anatomy

The liver is the largest internal organ in the human body, representing slightly less than 3 % of body weight, weighing 1,200–1,500 g, but receiving 25–30 % of the cardiac output. It is located in the right upper abdominal quadrant within the peritoneal cavity.

During weeks two to three of development, the gastrointestinal tract (GIT) arises from the endoderm of the trilaminar embryo. The three distinct portions, an anterior foregut, a central midgut, and a posterior hindgut ultimately contribute different components of the GIT. The foregut includes hepatic cells and bile ductules, gall bladder and common bile duct, pancreatic acinar and island cells, and duodenum. The liver and biliary tree appear late in the third week or early in the fourth week as the hepatic diverticulum, an outgrowth of the ventral wall of the distal foregut. The hepatic diverticulum subsequently divides into a small ventral part, the future gall bladder, and a larger cranial part, the liver primordium; the latter portion grows and differentiates into the parenchyma of the liver (hepatocytes) and the lining of the biliary ducts. The hepatocytes arrange into a series of branching and anastomosing plates in the mesenchyme of the transverse septum. These plates subsequently intermingle with vitelline and umbilical veins to form hepatic sinusoids. Besides contributing to the sinusoids, the splanchnic mesenchyme in the transverse septum also forms the stroma, the fibrous and serous coverings (liver capsule), the falciform ligament, and the blood forming, or hematopoietic tissue (Kupffer cells), of the liver. The connective tissue and smooth muscle of the biliary tract also develop from this mesenchyme. By the sixth week, the liver performs hematopoiesis (the formation of blood cells) and represents 10 % of the total weight of the fetus by the ninth week.

The liver is divided into two lobes: the right and the left, separated by the middle hepatic vein, which defines the imaginary line, the so-called Cantlie's line, from the middle of the gallbladder fossa and corresponding to the plane of the inferior vena cava (IVC), which runs posteriorly to the liver. The right and left lobes are each drained by a major vein (the right and left hepatic veins, respectively). The middle hepatic vein and these two veins drain into the IVC on the superior-posterior aspect of the liver. There is variation to the overall vascular drainage, and in some people, the left and middle hepatic veins become confluent prior to emptying into the IVC.

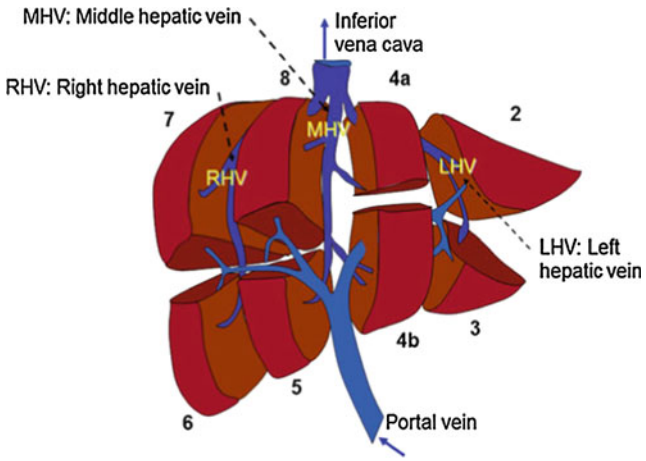

Fig. 2 The natural anatomy of portal vein flow and the right hepatic vein (RHV), middle hepatic vein (MHV), and left hepatic vein (LHV) drainage is utilized in the definition of hepatic segments; the caudate lobe (not shown here) represents segment 1

Using the anatomic location of the three hepatic veins, the liver has been divided into seven segments, based on the Couinaud classification system. Each lobe is divided into four segments, I through IV on the left and V through VIII on the right with segment I representing the caudate lobe (Couinaud 1992). Each segment has its own vascular inflow, vascular outflow, and biliary drainage (Fig. 2).

2.1.2 Vasculature

The liver receives dual blood supply from the portal vein (70 %) and hepatic artery (30 %). The hepatic artery is rich in oxygen, while the portal vein provides the liver with metabolite-rich but relatively poorly oxygenized blood. The portal vein takes its origin from the confluence of superior mesenteric vein and splenic vein, between the posterior surface of pancreatic neck and anterior surface of the IVC. The portal venous and hepatic arterial blood supplies parallel each other as they enter the portal triad and sequentially divide among the segments and subsegments of the liver.

The relationship of the liver to the portal vein is important in the understanding of portal hypertensive changes. Although the larger part of blood supply to hepatocytes is from the portal vein, the biliary system obtains all its supply from the hepatic artery. An injury to the hepatic artery therefore tends to have more severe effect on the biliary system than the hepatocytes. The portal vein is autoregulated, but the extent of arterial flow is partly dependent on the portal flow, such that situations reducing portal flow reflexively increase arterial flow. The mean pressure in the portal vein is 10 mm Hg compared to 90 mm Hg in the artery. However, the intrahepatic regulation ensures the arterial pressure does not extend into the sinusoids, which have a mean pressure of 5 mm Hg. Any pathologic process interfering with sinusoidal flow could have a far-reaching effect on this arterial pressure regulation and hepatic hemodynamics. This has relevance, as described in Sect. 3.3.2, in the pathogenesis of sinusoidal obstruction syndrome.

In summary, the liver receives dual arterial and venous blood supply, which flow through a system of sinusoids within the hepatic parenchyma in well-regulated pattern, to empty through small hepatic veins, that in turn drain into one of three major hepatic veins, and ultimately into the IVC. Details of the intrahepatic flow through the sinusoids are discussed in the next section—microanatomy.

2.2 Histology (Microanatomy)

The flow from the portal vein and hepatic artery enter the hepatic hilum soon after each divides into the right and left branches. Subsequent intrahepatic divisions create up to 1,000,000 interlobular branches of the portal vein and hepatic artery. The biliary system drains in the opposite direction but follows similar architecture, such that interlobular bile ducts (that drain bile canaliculi) progressively confluent to form the right and left hepatic ducts, which exit at the hilum, and fuse to become the common hepatic duct. The point where the cystic duct draining the gallbladder joins the common hepatic duct represents the beginning of the common bile duct, which eventually empties into the duodenum at the ampulla of Vater. Lymph flows in the same direction as bile. Thus, each interlobular portal tract consists of (at least) an arteriole, a venule, a bile duct, and lymphatic vessels enmeshed within a fibrous connective tissue, hence the term portal triad. Figure 3a shows the low magnification hepatic lobules and Fig. 3b shows the high magnification intralobular structure.

Surrounding the connective tissue is a single layer of hepatocytes running concentric to the triad and termed the limiting plate. The next layers of hepatocytes are arranged perpendicular to this plate running from the portal tract to the central vein (strictly a venule from its size). Separating the hepatocyte cords from each other is a system of sinusoids, lined by hepatocyte-specific fenestrated endothelial cells with a different immunophenotype from endothelial cells elsewhere in the body (see below). They function to regulate the passage of material between the sinusoids and subendothelial space that is in direct contact with hepatocytes. This perisinusoidal space (space of Disse) houses hepatic stellate cells (Ito cells) and native liver macrophages (the Kupffer cells). The stellate cells are storage site for vitamin A, and can become activated to assume myofibroblastic phenotype and function, playing significant role in fibrosis formation in most chronic liver injuries. After traversing the sinusoids, the vascular outflow proceeds to the

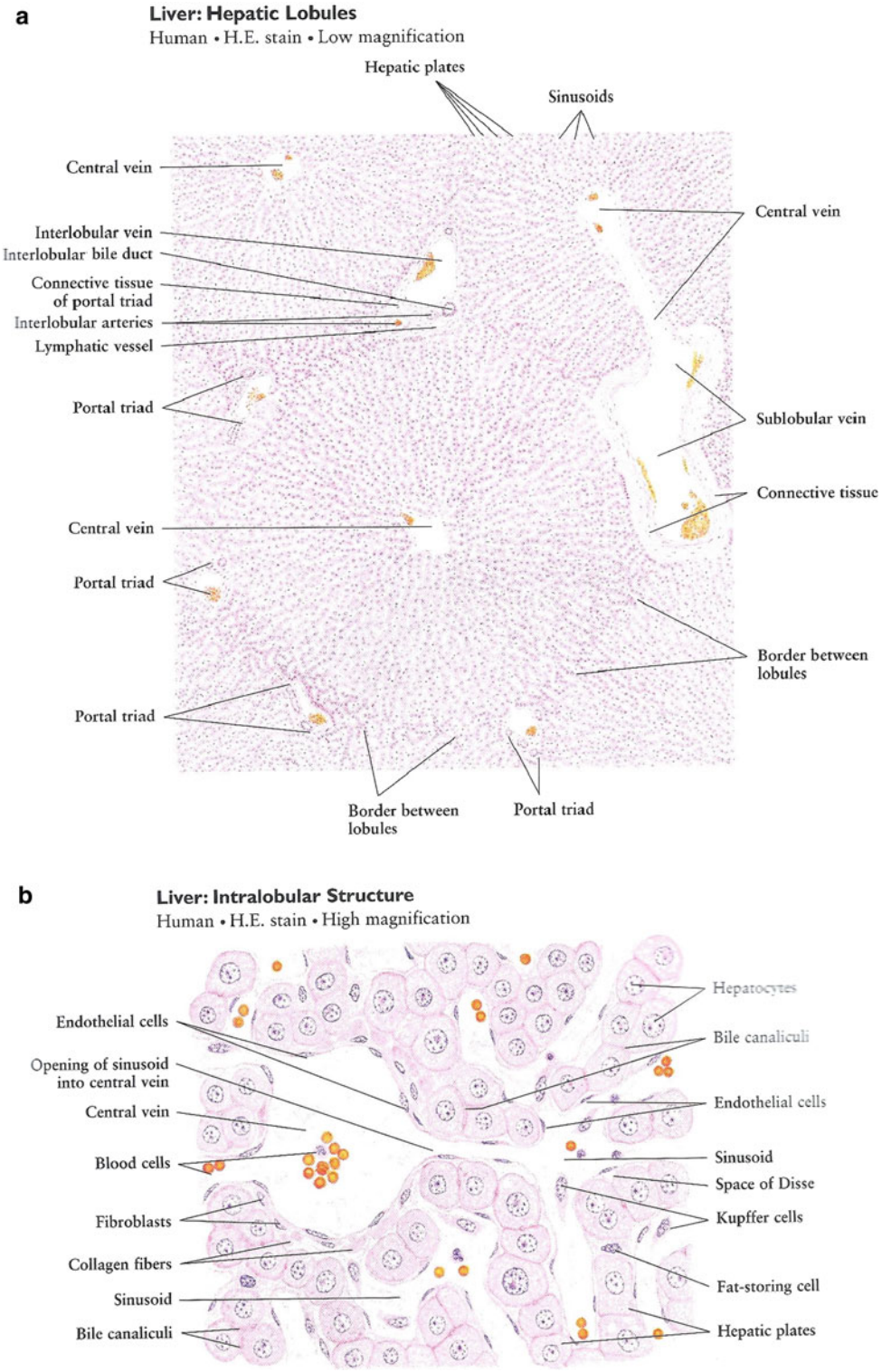

Fig. 3 Liver histology. **a** Low magnification. **b** High magnification (with permission from Zhang 1999)

central veins, the sublobular veins, and then to the supra-hepatic vein that ultimately drains into the IVC.

Endothelial cells, with two types of phenotypes, line the entire vascular system of the liver. The endothelial cells lining the portal veins, hepatic artery, hepatic venules, and hepatic veins exhibit systemic phenotype in that they are continuous and express among others, CD34 and factor VIII-related antigens, as would be expected elsewhere in the body. In contrast, the endothelial cells lining the sinusoids are fenestrated and do not express these antigens. In pathologic states such as neoplasms and cirrhosis, sinusoidal endothelium can revert to systemic phenotype (Couvelard et al. 1996).

3 Biology, Physiology, and Pathophysiology

3.1 Physiology (Functional Unit)

Traditionally, two structural systems have been considered as representing the functional unit of the liver, i.e., the smallest unit that represents the complete structure, function, and hemodynamics of the entire system: the acinar and the lobular systems. The lobule has a hepatic venule at its center with 3–6 vascular inflow portal triads arranged at the periphery of a polygonal unit (Fig. 3). Blood flows from the portal triad toward the central vein, and the oxygen concentration accordingly decreases toward the perivenous sinusoids. This does not truly represent the entire complex, as blood flows in the opposite direction to the lobular concept. For this reason, Rappaport defined the acinar concept as being more representative of the true function and hemodynamics of the liver (Rappaport 1976). The hepatic acinus includes the portal tract at its center, where blood and nutrients enter the unit and the central vein at the periphery or distal end, where the liver is drained. The hepatocytes closest to the portal tracts are functionally and metabolically different from the ones further away, around the hepatic venule (Jungermann 1988). Among these differences is their relative susceptibility to various forms of injury; for example the distal (peri-venular) hepatocytes are more susceptible to hypoxic/ischemic injuries than the more proximal hepatocytes. The proximal or periportal hepatocytes, also known as the zone 1 hepatocytes, are better oxygenized, but more susceptible to injury from some toxins that enter the liver via portal flow and are more concentrated at this zone. The distal hepatocytes in the unit are termed zone 3 hepatocytes, and those between zones 1 and 3, termed zone 2. Zones 1, 2, and 3 therefore correspond, respectively, to periportal, mid-zonal, and centrilobular (or perivenular) divisions of the lobular unit, as shown in Fig. 4. For most practical and descriptive purposes, the acinar unit is often utilized to describe the functional unit of the liver.

Within the liver, there are many functional subunits, with substantial redundancy.

3.2 Pathophysiology

3.2.1 Tissue, Cellular Mechanisms

The numerous redundant functional subunits within the liver allows the liver to endure substantial injury prior to development of any clinical sequelae. In noncirrhotics, surgical resection of a majority of the liver that leaves only a 20–25 % liver remnant has been shown to be well tolerated. Because of this redundancy, partial liver irradiation to high doses is possible using conformal radiation therapy if adequate normal liver parenchyma can be spared.

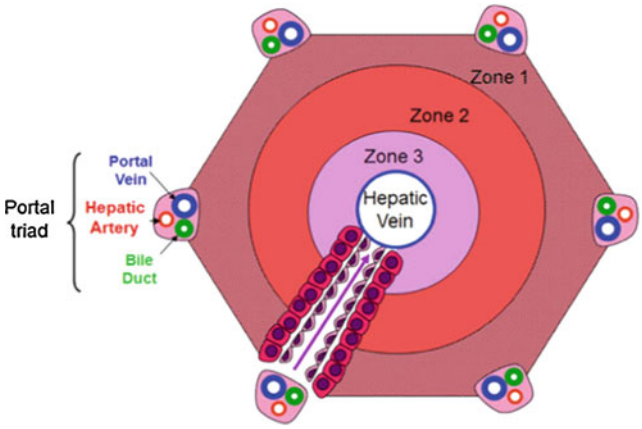

Fig. 4 Illustration of normal hepatic acinus illustration showing zones 1–3 as they relate to the portal tracts and hepatic vein. The arrow depicts direction of blood flow through the sinusoids

Due to the surplus of functional subunits in one liver, the architecture of the liver can be considered predominantly arranged "in parallel". Seriality in vascular and biliary function exists, as the vascular structures and the biliary system have many bifurcations throughout the liver that ultimately drain to main vessels or the common bile duct. Injury to the main vessels or common bile duct will have more adverse clinical consequence that injury to a distal branch. Furthermore, large vascular or biliary injury may alter the function of the liver associated with these structures. Thus the liver function itself may be considered mainly "in parallel", with potential for some "serial" function.

Regarding classic RILD, the underlying pathophysiology is poorly understood. However, injury to endothelial cells rather than hepatocytes has been postulated to be initiating, due partially to the timing of pathological changes observed in classic RILD (described in Sect. 3.2).

3.2.2 Morphological Appearance of RILD

The morphological appearance of classic RILD in humans is one of VOD, predominantly of the central and sublobular hepatic veins, with sparing of the periportal areas, larger hepatic veins, and hepatic arterial vasculature (Fajardo and Colby 1980; Reed and Cox 1966; Ogata et al. 1963) (Fig. 5c). While the lesion may affect anywhere from a portion of a lobule to the entire liver, it occurs strictly within the irradiated region and is sharply demarcated from adjacent unaffected areas of liver (Fig. 5a, b). Grossly, the involved liver appears markedly congested, and may contain areas of necrosis and parenchymal collapse in the center of larger involved regions.

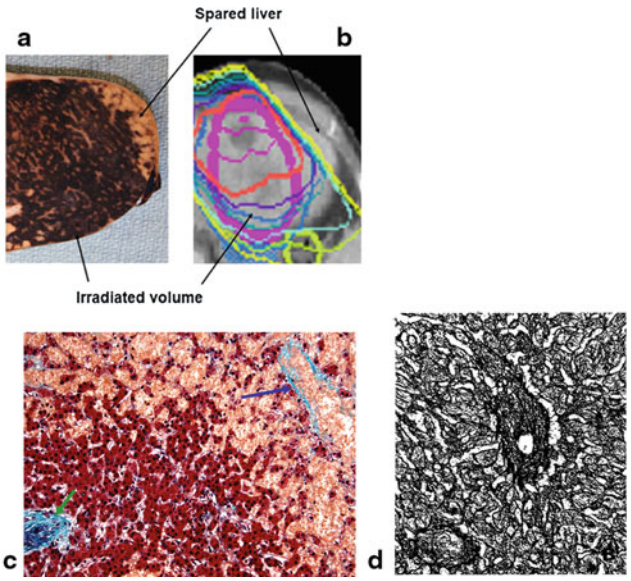

Fig. 5 **a** Gross photograph showing acute sinusoidal obstruction in resected left liver lobe following previous radiation therapy to a neoplasm (neoplasm not shown here), delivered 3 months previously. The sharp delineation of the change in the gross specimen is consistent with the radiation dose falloff, rather than anatomic regions. **b** Radiation plan: 30 Gy in 6 fractions (*yellow*), with sparing of the lateral left lobe. **c** Microscopy of acute sinusoidal obstruction in resected left liver lobe following radiation therapy; hepatic vein—*blue arrow*; portal tract—*green arrow*. The sinusoids and later the hepatic vein become prominent due to severe congestion (Trichrome stain, original magnification: 100x). (PDF Fig. 4). **d** Late fibrosis: typical centrilobular areas in moderately severe radiation-induced liver disease (RILD), fibrillary material (collagen) (with permission from Fajardo and Colby 1980[14])

In their classic description that established the features of RILD, Reed and Cox described in detail the progression of morphological changes that occur over the course of RILD (Reed and Cox 1966). In the early subacute period, typically the first month after RT, affected liver portions are markedly hyperemic, but display few venous lesions and only minimal evidence of outflow obstruction and hepatic cell loss. During the ensuing months, which correlate with the clinical presentation of RILD, veno-occlusive lesions become frequent and prominent, with severe vascular congestion and atrophy of centrilobular liver plates. The pathological hallmark of RILD, veno-occlusive lesions, are characterized by complete obliteration of central vein lumina by erythrocytes trapped in a dense network of reticulin and collagen fibers that crisscross the lumen of the central veins, sublobular veins, and centrilobular sinusoids. Fibrin appears to be deposited peripherally along the intimal walls of these vessels, rather than in center of the lumens as are collagen and reticulin. Collagen is present not only in the centrilobular veins, but appears to proliferate along the hepatic sinusoids and produce mild congestion in periportal areas as well. Centrilobular hepatocytes (zone 3) are largely absent, presumably due to hypoxic cell death secondary to vascular congestion. After approximately 4 months, vascular congestion resolves as the liver begins to gradually heal. Although asymptomatic, the hepatic architecture remains largely distorted, with persistent fibrosis of central veins, fibrous tracts bridging portal and central veins, and unrepaired lobular collapse prominent throughout the affected region (Fig. 5d).

A characteristic feature of RILD, which is not yet well studied in the other forms of VOD, is the deposition of fibrin strands with entrapment of platelets within the central veins as demonstrated by electron microscopy. The elevation of alkaline phosphatase more than the transaminases in classic RILD suggests that bile ducts or hepatic canaliculi may also be injured in irradiated livers.

Of note, thrombosis of larger hepatic veins, such as seen in Budd-Chiari syndrome, has been uncommonly seen following liver irradiation (Rahmouni et al. 1992). However, radiation-induced thrombosis is typically not associated with centrilobular coagulative necrosis and clinically does not usually induce jaundice, which is often seen in patients with Budd-Chiari syndrome.

3.2.3 Animal Models

The pathogenesis of RILD is difficult to investigate because of the lack of a suitable animal model. Rat (DeLeve et al. 2002), mice (Tabbara et al. 2002), dog (Reiss et al. 2002; Bearman 2001), and rhesus monkey (Shulman et al. 1980) models studied to date do not develop a similar pathology or clinical syndrome to that seen in humans (the VOD of classic RILD). However, the murine and rodent microvascular endothelial cells are sensitive to radiation injury (Shulman et al. 1987). Furthermore, perivenous atrophy of hepatocytes has been noted in rodent models of RILD, despite a lack of central vein occlusion by platelet thrombi (Shulman et al. 1994).

Geraci and colleagues first reported that rats receiving whole liver irradiation in excess of 25 Gy developed liver dysfunction after a latent period of 35–40 days (Geraci et al. 1991). In their study, hepatocellular injury was evident by elevations in AST, ALT, alkaline phosphatase, and ^{131}I rose bengal retention, an indicator of hepatobiliary clearance. Morphologically, these rats appeared to develop a pathology that somewhat resembled the VOD described in humans, with venous outflow obstruction by collagen deposition, sinusoidal vascular congestion, interstitial fibrosis, and focal necrosis of centrilobular hepatocyte (Geraci et al. 1991). However, no studies to date of hepatic irradiation in rodents by other investigators have successfully reproduced these pathological findings. This may be due to the fact that unless the entire liver is irradiated, even a small spared portion can rapidly regenerate and prevent

the clinical syndrome of RILD (Geraci et al. 1991). Thus, despite the promise of Geraci's reports, a reproducible rodent model that mirrors human RILD remains elusive.

3.2.4 Viral Hepatitis

Another mechanism thought to contribute to the pathogenesis of nonclassic RILD is the subclinical or ongoing cirrhosis of the liver associated with hepatitis B virus (HBV). Most patients undergoing irradiation of the liver in East Asia are HBV carriers. Cheng et al. found that chronic infection with HBV was associated with a higher risk of developing nonclassic RILD (which presented as elevated serum transaminases) in a univariate analysis of patients treated with radiation (Cheng et al. 2002, 2004a). After stratifying their patients, they noted that the HBV carrier group had a shifted normal tissue complication probability curve, with a reduced tolerance compared to the noncarrier group. These arguments suggested the possibility of a unique mechanism (e.g. HBV reactivation) in the development of non-classic RILD (and reduction in liver dose tolerance) in carriers of HBV.

In general, the reactivation of viral hepatitis in HBV carriers can occur without a causative factor as a sporadic event (Tsai et al. 1992). Hepatic venulitis can be seen as part of the picture in viral hepatitis, and other causes of severe hepatitis, leading to significant injury and subsequent loss of affected venules. This could subsequently produce sinusoidal congestion. Because the injury is often patchy, the sinusoidal congestion usually is minimal, as the liver is capable of diverting flow toward adjacent veins with no or milder injury. Chemotherapeutic agents have been associated with HBV reactivation (Yeo et al. 2000). The reactivation of HBV is implicated as the mechanism why HBV patients may have a reduced tolerance to irradiation, though only recently has data been collected to confirm viral reactivation after liver irradiation. In the 2004 Cheng et al. report, 2 of the 17 patients who developed RILD were examined for reactivation of HBV, and both patients demonstrated serologic evidence of viral reactivation (Cheng et al. 2004b). In a separate report by Cheng et al., it was shown that 6 of 8 patients with gastric cancer who developed nonclassic RILD were chronic HBV carriers, and 4 of the 6 carriers had serologic evidence of viral reactivation following adjuvant chemotherapy and radiation therapy (Cheng et al. 2004a).

Kim et al. compared liver irradiation in a group of patients with chronic hepatitis B requiring antiviral treatment at the time of irradiation versus a group of HBV carrier patients without active disease. They found that reactivation of HBV and nonclassic RILD, though not necessarily together, occurred more commonly in the latter group (Kim et al. 2007).

Although it has become established that reactivation of HBV may occurs after liver irradiation, the mechanism is not yet known. Radiation could directly reactivate HBV residing in a hepatocyte, or it may be due to the effect of radiation on nearby nonparenchymal cells (Chou et al. 2007). The direct effect and the so-called bystander effect were tested by Chou et al. by transferring various conditioned media in vitro. They found that the direct effect of radiation on hepatocytes, normal or cancerous, did not show reactivation of HBV. However, transferring conditioned medium of irradiated noncancerous hepatocytes or irradiated endothelial cells resulted in HBV DNA replication (Chou et al. 2007). They went on to show that IL-6 that is released from endothelial cells after irradiation, suggesting that radiation-induced reactivation of viral hepatitis B probably occurs due to a bystander effect of IL-6.

3.3 Biology (Molecular Mechanisms of RILD)

3.3.1 Sinusoidal Endothelial Injury

It has been traditionally postulated that the initiating lesion of VOD in RILD occurs at the level of the sinusoidal endothelium. Electron microscopy studies of affected liver in classic RILD have revealed fibrin deposits throughout the central veins and adjacent sinusoids. These findings led to the supposition that damage to sinusoidal endothelial cells (SECs) and central vein endothelium initiates activation of the coagulation cascade, leading to accumulation of fibrin in the central veins and hepatic sinusoids (Lawrence et al. 1995). It is thought that deposited fibrin serves as a foundation for the proliferation of reticulin and collagen, which eventually occludes the vessel lumen. The trapping of erythrocytes in this collagen meshwork produces vascular congestion and decreased oxygen delivery to the central zone, which is inherently sensitive to hypoxia due to the physiological oxygen gradient within the hepatic lobule. This hypoxic milieu presumably results in death of centrilobular hepatocytes and atrophy of the inner hepatic plate, producing the hepatic dysfunction observed clinically in RILD (Lawrence et al. 1995).

3.3.2 Sinusoidal Obstructive Syndrome

A similar pathological entity to the VOD of classic RILD, named sinusoidal obstructive syndrome (SOS) to distinguish it from other forms of VOD, has been observed in several clinical scenarios. Classic causes of SOS include ingestion of herbal teas or foods containing pyrrolizidine alkaloids, prolonged immunosuppression with azathioprine, and a wide range of chemotherapeutic agents, including dacarbazine, and cyclophosphamide. The most common cause of SOS is myeloablative chemotherapy or

combination chemoradiotherapy for bone marrow transplantation (BMT).

Studies of monocrotaline-induced SOS models have delineated a clear sequence of events by which sinusoidal and venous obstruction occurs in rats (DeLeve et al. 1999). In this model, the earliest observed changes appear to be loss of SEC fenestrations and appearance of gaps in SEC endothelium (DeLeve et al. 1999). Digestion of extracellular matrix on the abluminal side of SECs membrane causes SECs to "round up" and facilitates penetration of red blood cells into the underlying space of Disse, leading to dissection of the endothelial lining and narrowing of the sinusoidal lumen (DeLeve et al. 1999, 2003). The dissected sinusoidal endothelium embolizes and obstructs downstream sinusoids and central veins, producing hepatic vascular congestion. Clinical signs of SOS can occur in the absence of central vein occlusion, implying that sinusoidal injury is sufficient to cause clinically significant microcirculatory hepatic dysfunction, as confirmed in this animal model of SOS. By comparison, central vein obstruction is considered a prominent and defining pathological feature of classic RILD, presumably occurring secondary to luminal deposition of fibrin, reticulin, and collagen that traps of erythrocytes and produces vascular congestion and hepatic hypoperfusion.

The earliest morphological change observed in human studies of SOS is edematous widening of the subendothelial space of central and sublobular veins by fragments of erythrocytes (RBCs) and cellular debris (Shulman et al. 1980, 1987, 1994). This is accompanied by sinusoidal dilation and engorgement, erythrocyte penetration into the space of Disse, and necrosis of perivenular hepatocytes (DeLeve et al. 2002). Similar to the animal models, the sinusoidal pathology in SOS is typically more prominent than the central vein changes, an important difference from classic RILD. Sinusoidal injury is thought to be the responsible for the hepatocellular damage and clinical signs of SOS. This hypothesis is supported by findings that clinical signs of SOS correlate with perivenular lesions in the absence of venous occlusion, and that, in one series, 45 % of patients with mild-to-moderate SOS and 25 % of patients with severe disease lacked central vein obstruction on autopsy (Shulman et al. 1994). However, central vein involvement has been shown to correlate with both ascites and disease severity, suggesting that while not requisite to disease development, central vein obstruction significantly exacerbates circulatory impairment and hepatic dysfunction in SOS (Shulman et al. 1994; Rollins 1986).

As in classic RILD, deposition of fibrin and collagen has been observed in SOS, although reports of this finding vary. The fibrosis occurs in the zone-3 sinusoids and can range from mild-to-severe (cirrhotic) depending on the severity and extent of sinusoidal injury. Shulman et al. compared autopsy samples of liver tissue from BMT patients with VOD and without VOD by immunohistochemical analysis (Shulman et al. 1987). Of 11 patients 9 with early VOD demonstrated dense factor VIII staining of central veins, compared to only 2 out of 12 patients without VOD, suggesting activation of the coagulation cascade in the development central vein obstruction in SOS. The observation in this study that positive staining for fibrinogen was present in 4 out of 4 patients with early VOD, compared to 0 out of 4 patients without VOD, supports a role for clotting in the development of early SOS. Furthermore, extensive luminous obliteration by collagen in late VOD was identified in central veins (2/4 pts) and centrilobular sinusoids (3/4 pts), as compared to the localization of collagen in early VOD to only sinusoids (2/3 pts) and not central veins (0/3 pts) (Shulman et al. 1987). Although derived from a small patient population, the temporal differences in these findings between early and late VOD support the theory that sinusoidal endothelial injury initiates the pathogenic cascade in SOS, and that consequent deposition of fibrin serves as a scaffolding upon which collagen accumulates and obstructs sinusoids and downstream central veins.

Other studies of patients undergoing myeloablative BMT (Sartori et al. 2005; Brooks et al. 1970) provide anecdotal evidence for the involvement of clotting cascade activation of the development of SOS. In one study of 53 consecutive pediatric patients receiving BMT, children who developed VOD had significant increases in plasminogen activator inhibitor type I, tissue plasminogen activator, and D-dimer and significant decreases in prothrombin time, antithrombin, and α2-antiplasmin at either 2 days prior to or 1 day after clinical diagnosis of VOD, as compared to patients who did not develop VOD (Sartori et al. 2005). Several retrospective analyses in BMT patients have demonstrated less frequent symptoms and lower incidences of SOS in cohorts receiving prophylaxis therapy with heparin, defibrotide, and/or prostaglandin E1, providing further support for a causal or pathogenic role of thrombosis and hypercoagulability in the development of SOS (Chalandon et al. 2004; Rosenthal et al. 1996; Simon et al. 2001). Given the widespread morphological similarities between classic RILD and SOS, one may speculate that aberrant coagulation cascade activation may also play a role in the pathogenesis of classic RILD, although no clinical studies to date have adequately addressed this possibility.

Despite their pronounced etiological and clinical differences, the morphological similarities between VOD and SOS suggest that SOS may be an important disease model from which we can gain a better understanding of classic RILD. Analogous to the postulated mechanism of RILD, liver sinusoidal endothelial cells appear to be the primary target of drugs that produce SOS (DeLeve 1994, 1996, 1998). Of particular significance is the fact that all of these

compounds are (a) detoxified by glutathione (GSH) and (b) selectively more toxic to SECs than to hepatocytes (DeLeve 2007). Depletion of GSH due to metabolism of each of these compounds precedes SEC toxicity in vitro, suggesting that metabolite conjugation by GSH may play a protective role in preventing SEC damage and SOS caused by these drugs (DeLeve 1994, 1996, 1998).

In summary, it is plausible that, as in SOS, damage to SECs may precede the development of central vein obstruction in classic RILD. In SOS, central vein involvement appears to worsen the severity of disease (Shulman et al. 1994; Rollins 1986). It is equally plausible that the scenario is analogous for radiation-induced liver damage, as injury limited to SECs may produce only subclinical disease, whereas obstruction of downstream central and sublobular veins results in clinically manifest RILD.

3.3.3 Activation of Hepatic Stellate Cells

In addition to endothelial cell damage, several other mediators of hepatic damage are thought to contribute to the development of RILD. Hepatic stellate cell (HSC) activation, in particular, has been observed in patients who developed severe congestive changes characteristic of RILD in the months following RT for biliopancreatic cancer, prior to the development of fibrosis (Sempoux et al. 1997). In a study of six such patients by Sempoux and colleagues, activated HSCs, characterized by expression of the α-isoform of smooth muscle actin (α-SMA), were variably identified throughout congested irradiated areas and found within thickened central vein walls and adjacent to or within congested centrilobular sinusoids (Sempoux et al. 1997), while activated HSCs were not present in all samples from all patients and were unevenly distributed in congested areas, their presence did appear to coincide with severity of fibrosis and architectural distortion. α-SMA positive cells were also notably absent from nonirradiated areas, suggesting an association between hepatic irradiation and stellate cell activation. While the small patient population ($n = 6$) and lack of statistical analysis limits our ability to draw any conclusions from this study, the observations of stellate cell activation in RILD are nonetheless intriguing and warrant further investigation.

3.3.4 Transforming Growth Factor-β

The transforming growth factor-β (TGF-β) family consists of the TGF-β1, TGF-β2, and TGF-β3 precursor isoforms (Blobe et al. 2000; Khalil 1999). The propeptides are cleaved by proteolytic cleavage from the active TGF-β peptide growth factor that exists functionally as a dimer held together by disulfide bonds. TGF-β is ubiquitous as nearly every cell in the human body produces TGF-β and has receptors for it (Blobe et al. 2000). TGF-β is integral in the interaction between cells and the extracellular matrix in the processes of inflammation, immune response, and wound healing. It is also important in cell cycle regulation and in the apoptotic pathway. The reactive interaction between parenchymal cells, nonparenchymal cells, and the extracellular environment occurs through the language of cytokines. TGF-β proves to be one of the most important cytokines associated with tissue injury and wound healing (Amento and Beck 1991; Barcellos-Hoff 2005a, b; Barcellos-Hoff et al. 2005). The pathogenesis of RILD, though still unclear, may have less to do with direct parenchymal damage and more likely is a result of the tumor microenvironment as a result of irradiation.

As such, TGF-β has been implicated in playing a role in the fibrogenesis leading up to RILD. Fibrin deposition in the sinusoids and subendothelial space has been shown to occur after liver irradiation (Fajardo and Colby 1980). After a stable period of fibrin deposits, fibroblasts migrate to the region of injury and undergo proliferation and production of collagen under the influence of TGF-β (Amento and Beck 1991). TGF-β is not necessarily associated with radiation injury; rather, it is present in a non-specific manner in many types of liver disease, such as cirrhosis, chronic hepatitis, or chemotherapy-induced liver disease (Anscher et al. 1993; Castilla et al. 1991).

Anscher et al. described the dose dependence of the level of TGF-β in irradiated liver; they also showed that the level of TGF-β in hepatocytes was higher in the region of more extensive fibrosis (Anscher et al. 1990). After creating an association with TGF-β, dose, and fibrosis, they were able to identify a temporal or cause-and-effect relationship by demonstrating a fibrotic reaction in healthy rat livers after injection with TGF-β (Anscher et al. 1990). Rodent models of VOD and RILD have been elusive (as described in Sect. 3.2.3). Anscher and colleagues reported that the level of TGF-β in normal human hepatocytes was higher than that in normal rat hepatocytes, raising a possible reason why humans have a greater tendency to develop VOD as compared to rats (Anscher et al. 1990). The same group reported separately that patients who received induction chemotherapy prior to BMT and high-dose chemotherapy and developed VOD after treatment had significantly higher levels of pretransplantation TGF-β as compared to patients who did not develop VOD and to normal controls (Anscher et al. 1993).

TGF-β may not be the only factor contributing the mechanism of RILD, but it is certainly significant in the pathogenesis. Furthermore, it is a compelling hypothesis that TGF-β may play a role in determining why humans develop VOD more readily than other animal models.

3.3.5 Other Cytokines

Aside from TGF-β, there are a number of other cytokines and downstream reactants that participate in the response to

tissue injury. The inflammatory condition that leads to cytokine release is typically associated with injury (e.g. burns, trauma), exposure to endotoxins, or exposure to foreign materials (e.g. infection). The importance of the inflammatory response in these conditions is in recruiting leukocytes to the site of stress so that the host may react to the damage. Gourmelon et al. has shown that a similar cytokine release pattern occurs in nonhuman primates subsequent to whole body irradiation (Gourmelon et al. 2005). A number of authors have similarly demonstrated the release of inflammatory cytokines with irradiation of various organs or cell types (Fedorocko et al. 2002; Linard et al. 2003; Beetz et al. 1997; Meeren et al. 1997; Hosoi et al. 2001; Ishihara et al. 1993).

Similarly, Christiansen et al. showed that irradiation of rat liver in vivo induces upregulation of proinflammatory cytokines IL-1-beta, IL-6, and tumor necrosis factor alpha (Christiansen et al. 2007). The same group demonstrated that in vitro irradiation of isolated hepatocytes alone showed no effect versus irradiation of hepatocytes in a medium supplemented with the proinflammatory cytokines, which induced the upregulation of hepcidin, an acute phase reactant (APR). Moriconi et al. were able to show that hepatocytes had upregulation of chemokines after irradiation in vivo (Moriconi et al. 2008). Similarly, they showed that in vitro hepatocytes had upregulation of these chemokines only in the presence of proinflammatory cytokines. Although higher dose tolerance has been shown for partial liver irradiation (Dawson and Ten Haken 2005), the whole liver is sensitive to irradiation, with greater than a 5 % risk of toxicity above doses of 30–35 Gy in 2-Gy fractions (Ingold et al. 1965; Emami et al. 1991; Austin-Seymour et al. 1986). Conversely, hepatocytes irradiated in vitro have been demonstrated to be relatively radioresistant (Jirtle et al. 1984; Jirtle et al. 1982; Jirtle et al. 1981; Alati et al. 1988, 1989a, b). Therefore, hepatocytes irradiated in vivo or in a medium of proinflammatory cytokines demonstrate a weakened state that confers the overall radiosensitivity of the whole liver. The proinflammatory cytokines are not released from the hepatocytes themselves, but are released from nonparenchymal cells (i.e. Kupffer cells and SECs) and via a paracrine affect can induce hepatocyte production of APRs (Christiansen et al. 2007; Moriconi et al. 2008; Ramadori and Armbrust 2001).

In other types of liver injury, chemokines play a central role in the recruitment of leukocytes (Ley 1996; Mehendale 2005), which likely contribute to the development of fibrosis. However, despite the upregulation of chemokines from hepatocytes after irradiation, Moriconi et al. did not observe significant leukocyte recruitment in the liver (Moriconi et al. 2008).

4 Clinical Syndromes

4.1 Clinical Endpoints

A variety of endpoints characterize radiation-induced liver injury. It is sometimes useful to categorize the endpoints, albeit somewhat arbitrarily, as shown in Table 2. Note that the cytokine changes have been demonstrated primarily in preclinical models, and are not ready to be used routinely in a clinical setting.

4.1.1 Liver Toxicity Subtypes

Liver toxicity has not always been separated into "classic" and "non-classic" RILD in the literature, which has contributed to some challenges in understanding the different pathophysiology and the dependence on radiation dose and volume for different liver toxicities that may occur following irradiation. Below, potential liver toxicities that may occur following liver irradiation are described. Of note, "non-classic RILD" includes any serious liver toxicity that may not fit into the other categories, and with time it is possible that different nonclassic RILD toxicities may be better understood and separated as entities of their own.

4.1.1.1 Classic RILD

As described previously, the most commonly studied hepatic toxicity following liver irradiation is classic RILD, a clinical syndrome mimicking VOD following stem cell transplantation, presenting with anicteric ascites and hepatosplenomegaly (Lawrence et al. 1995). RILD typically occurs between 2 weeks and 3 months after the completion of irradiation. Patients typically present with fatigue, rapid weight gain, increased abdominal girth, and, occasionally, right upper quadrant pain or discomfort, in the absence of icterus or jaundice. Ascites and hepatomegaly may be seen on physical examination. Laboratory findings usually consist of significant elevations in alkaline phosphatase (3–10 times upper limit of normal) and mildly increased aspartate transaminase (AST) and alanine transaminase (ALT) levels ($\sim$2 times upper limit of normal), with other liver function tests, including bilirubin, within normal limits (or at baseline pre treatment levels). RILD is defined in the absence of intrahepatic progression of cancer, as progressive cancer may mimic or mask RILD.

The clinical manifestations and course of RILD differ significantly from that of acute liver failure. Patients in acute liver failure typically present with more acute symptoms of nausea, vomiting, abdominal pain, dehydration, and jaundice. While RILD can progress to fulminant hepatic failure, particularly in the presence of underlying

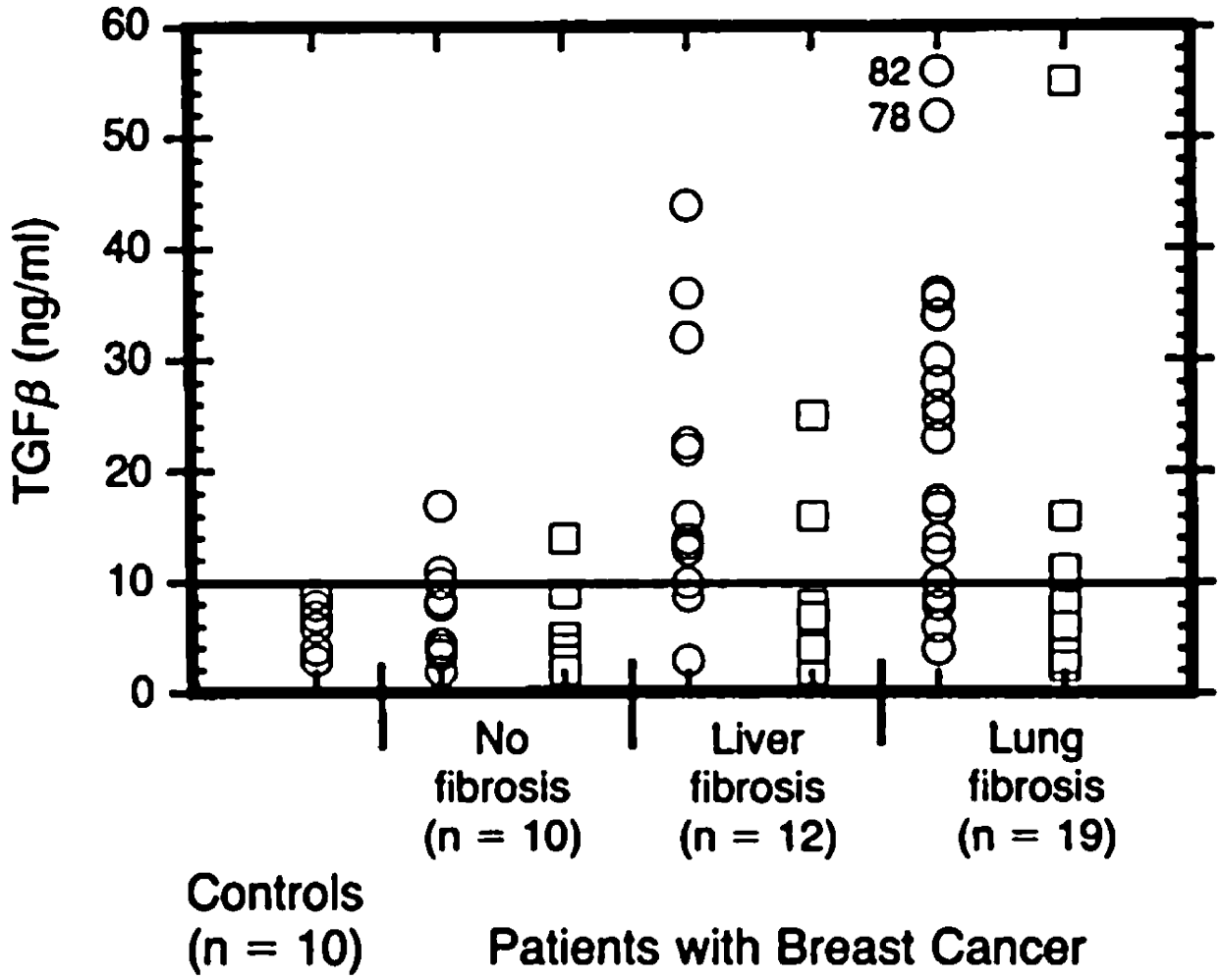

Fig. 6 Transforming growth factor β as a predictor of liver and lung fibrosis after autologous bone marrow transplantation for advanced breast cancer by Anscher et al. (1993). Individual TGFβ plasma concentrations in the four study groups. Healthy blood donors served as controls. One roup of patients did not have pulmonary fibrosis or hepatic veno-occlusive disease after high-dose chemotherapy and autologous bone marrow transplantation (no fibrosis); the two other groups had either hepatic veno-occlusive disease (liver fibrosis) or pulmonary fibrosis (lung fibrosis). TGFβ was measured before (*circles*) and after (*squares*) high-dose chemotherapy and transplantation (Anscher et al. (1993) shows the timing of the regimens). The *solid horizontal line* indicates the value (10 ng per milliliter, or 2 SD above the mean value determined in the controls) that was used as a cutoff point to determine the ability of pretransplantation TGFβ measurement to predict the development of hepatic or pulmonary toxicity after transplantation. To convert values for TGFβ to millimoles per liter, multiply by 4×10^{-8} (with permission from Anscher et al. 1993)

hepatic dysfunction, patients rarely present in acute liver failure. Figure 6 outlines the clinical workup, differential diagnosis, and management of classic RILD.

4.1.1.2 Nonclassic RILD

Nonclassic RILD is defined as elevated liver transaminases more than five times the upper limit of normal or CTCAE grade 4 levels in patients with baseline values more than five times the upper limit of normal within 3 months after completion of RT or a decline in liver function (measured by a worsening of Child-Pugh score by 2 or more), in the absence of classic RILD or progression of intrahepatic cancer (Pan et al. 2008). This endpoint has been described most commonly in patients with hepatocellular carcinoma who have compromised baseline liver function (hepatitis B infection, Child-Pugh B or C liver function) (Cheng et al. 2003; Liang et al. 2006).

A confounder of classic and nonclassic RILD, especially in populations with pre-existing liver dysfunction, is the baseline decline in liver function within this population that occurs with time due to pre-existing liver disease and/or progressive liver cancer. In a randomized trial in unresectable hepatocellular carcinoma of placebo versus Sorafenib, a multitarget kinase inhbitor, there was a 54 % rate of serious adverse events among the placebo group due to progression of cirrhosis and/or cancer (Llovet et al. 2008).

Table 1 Child-Pugh scoring system to assess severity of liver disease or toxicity

Criterion	1 point	2 points	3 points
Bilirubin (total)	<2 mg/dL	2–3 mg/dL	>3 mg/dL
Albumin	>3.5 g/dL	2.8–3.5 g/dL	<2.8 g/dL
INR	<1.7	1.71–2.20	>2.20
Ascites	None	Controlled with medication	Refractory
Hepatic encephalopathy	None	CTCAE grade I–II (or controlled with medication)	CTCAE grade III–IV (or refractory)

Points	Class	2-year survival (%)
5–6	A	85
7–9	B	57
10–15	C	35

INR international normalized ratio, *CTCAE* common terminology criteria for adverse events

Table 2 Representative endpoints of radiation-induced liver injury segregated as clinical vs. subclinical and global vs. focal, as shown

	Focal	Global
Subclinical	Regional changes on contrast CT Regional changes on contrast MR Regional changes in MR SPECT	Ascites Hepatosplenomegaly Increased ALP Increased liver enzymes (ALT, ALP) Increased Hepatitis B antigen Thrombocytopenia Changes in albumin, bilirubin, and INR Changes in indocyanine green (ICG) extraction Elevated TGF-β Elevated IL-1β Elevated IL-6 Elevated TNF alpha Elevated N-terminal peptide of type III procollagen propeptide Reduced protein C
Clinical	Fibrosis in critical region of liver, e.g., common bile duct leading to biliary obstruction	Increased abdominal girth Right upper quadrant pain Weight gain Fatigue Edema Confusion Encephalopathy

Nontheless, liver function (e.g. Child-Pugh score) is an important endpoint to report following treatment, as a decline in liver function is clinically relevant, whether it is due to progressive liver cancer, underlying cirrhosis or treatment. Thus, in addition to reporting nonclassic RILD in patients without progression of liver disease, any change in liver function (as measured using Child-Pugh score, Table 1) at 3 months following irradiation is recommended to be reported in all patients irradiated, including patients with progressive disease.

4.1.1.3 Reactivation of Hepatitis B Virus

Some patients who develop elevation of their liver enzymes, as described in Sect. 4.1.2, likely had hepatitis B reactivation induced by irradiation (Cheng et al. 2004a). Reactivation of HBV has now been described following liver irradiation in animal models and in patients. Reactivation of HBV can occur following chemotherapy, and thus, it is likely more common following combined chemotherapy and radiation in HBV carriers.

Patients planned to be treated with radiation therapy should be considered for tested for hepatitis B surface antigen (HBsAg) and anti-HCV. If either test is positive, further confirmatory testing should be done including HBV DNA or HCV RNA, and a referral to a hepatologist is recommended for treatment of viral hepatitis prior to irradiation.

4.1.1.4 Post Transplant Veno-Occlusive Disease

VOD is a frequent, serious, and often life-threatening complication of hematopoietic stem cell or bone marrow transplantation. It is believed to be caused by hepatic

endothelial cell injury from the high-dose cytoreductive conditioning regimens used during stem cell and bone marrow transplant protocols, often in combination with total body irradiation (TBI) (DeLeve et al. 2002; Bearman et al. 1993). Hepatocytes in zone 3 of the liver acinus are also injured by direct chemotherapy toxicity and ischemia due to endothelial clotting in the terminal hepatic venules.

Patients present with hyperbilirubinemia, fluid retention, and hepatomegaly. VOD has been defined as bilirubin $\geq$2.0 mg/dL, weight gain $\geq$2.5 % from pretransplant weight, and hepatomegaly and/or right upper quadrant pain, occurring within 2 weeks of transplantation, in the absence of other explanations for these signs or symptoms. The primary difference between transplant-associated VOD and RILD is the rapid elevation of bilirubin which may occur in transplant VOD within days following chemotherapy or TBI. Risk factors for VOD include previous hepatitis, mismatched or unrelated donor transplants, and high-dose chemotherapy regimens (i.e. high-dose Cyclophosphamide, or Cyclophosphamide and Busulfan). Interestingly, the use of TBI and the doses used in preparative regimens do not appear to be strongly associated with the risk of VOD occurring (Ganem et al. 1988).

VOD occurs in up to 50 % of patients following stem cell transplantation. 50 % of cases are irreversible and can lead to multiorgan failure. Disease prognosis generally depends on the degree of liver injury and the resulting severity of the hepatic dysfunction. Mild disease may not develop liver failure, and may reverse with supportive treatment. Moderate VOD includes evidence of liver dysfunction, and treatment with diuretics for fluid retention, and analgesics for right upper quadrant pain are often required. Fifty percent of patients present with severe and life-threatening VOD. These patients have the most dramatic rises in serum bilirubin, the fastest weight gain, the highest rates of ascites, and the most severe hepatic dysfunction. Prevention of VOD with heparin, prostaglandin E, and ursodeoxycholic acid have not definitively been shown to prevent or mitigate transplant-related VOD. Treatment with supportive care does not usually alter the course of this toxicity, and these patients often die of severe renal and cardiac failure. The day +100 post stem cell transplant mortality for these patients approaches 100 % (Bearman et al. 1993).

4.1.2 Grading of Toxicity

The Cancer Therapy Evaluation Program, Common Terminology Criteria for Adverse Events (CTCAE), Version 3.0, grades hepatobiliary toxicity according to clinical criteria including jaundice, asterixis, and encephalopathy or coma for grades 2, 3, and 4, respectively. These serious adverse events are rare following radiation therapy. Acute changes in liver enzymes or liver function tests are far more common during and/or following radiation therapy. Such liver enzyme abnormalities are classified under the CTCAE metabolic/laboratory category.

The Child-Pugh scoring system to assess liver dysfunction is based on an assessment of the clinical and laboratory parameters shown in Table 1. It can be used to characterize baseline liver function and also post-treatment changes in liver function.

4.2 Detection (Liver Function Tests)

4.2.1 Serum Markers

Assessment of liver function is an important component of evaluation of patient with liver cancer or other cancers in whom radiation therapy may be used for treatment. Serial measures of liver function are also useful in estimating the severity of radiation toxicity, and in predicting survival following development of classic or non-classic RILD. Hepatic synthetic function is assessed by measurement of serum albumin, bilirubin, and prothrombin time, which are critical components of the Child-Pugh scoring system. Decrease in platelet count and white blood cell counts may reflect the degree of portal hypertension and associated hypersplenism.

Other tests such as isocyanine green retention and 99m-Tc GSA (diethylenetriamine-penta-acetic acid-galactosyl human serum albumin) scintigraphy have been described as more specific indicators of hepatic reserve in preparation for resection, but have not convincingly surpassed the Child-Pugh classification as a predictor of post-operative complications and liver failure.

4.2.2 Indocyanine Green Clearance

The pathophysiology of RILD, as described in Sect. 3, leads to portal venous congestion and thereby altered vascular outflow from the liver. Cao et al. concluded that hepatocyte function was altered in the area of hypoperfusion using an indocyanine green (ICG) extraction study (Cao et al. 2008). While ICG clearance has been used as a measure of liver function, there have been discrepancies when compared with histological findings. ICG is taken up from plasma almost exclusively by hepatocytes, and subsequently secreted into bile. However, this function of hepatocytes does not measure the synthetic function or conjugative abilities of hepatocytes. Furthermore, ICG analysis measures whole liver function, and it is unable to identify specific regions of diminished functionality. Therefore, the outcome of the ICG test ultimately defines whether perfusion of the whole liver is adequate, where functionality of one portion of the liver can overshadow the dysfunction of another part of the liver. A more meaningful analysis would be to measure the function of the irradiated portion of the liver.

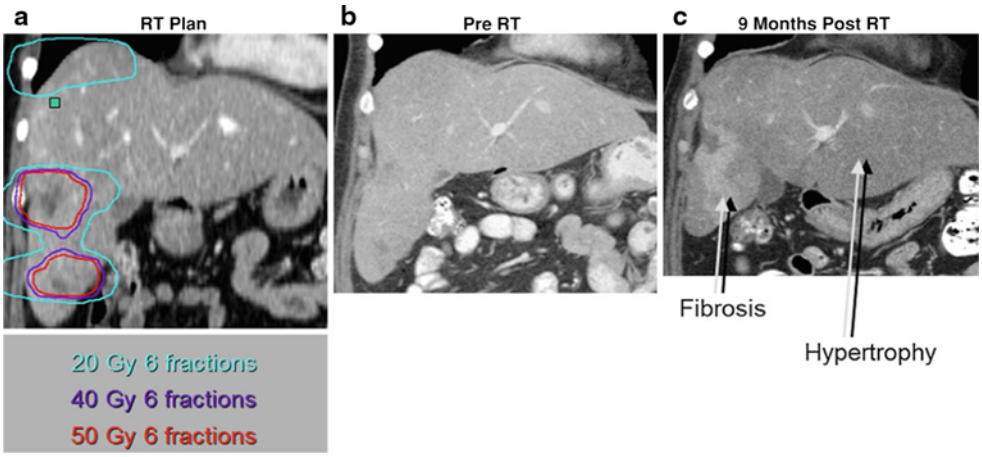

Fig. 7 Coronal views of preradiation therapy CT scans, with **a** and without **b** the radiation dose distribution shown, of a patient with multiple liver metastases, compared to CT 9 months following radiation therapy **c**, with fibrosis occurring in the liver irradiated to high doses and hypertrophy of the spared left lobe

4.3 Diagnosis (Imaging)

Focal changes in irradiated liver were documented on scintillation scanning as early as 1967 (Concannon et al. 1967). Changes in computed tomographic (CT) and MRI contrast enhancement have been seen within regions of the liver irradiated to high doses (Herfarth et al. 2003). Ultimately, the liver volume irradiated to high doses becomes fibrotic while the spared liver hypertrophies, as shown in Fig. 7. The threshold doses for these effects is a topic of ongoing research.

Characterizing RILD by noninvasive imaging has been challenging and the techniques are evolving. The CT findings of RILD were first described in a report of three patients who received partial liver irradiation (Jeffrey et al. 1980). The post-irradiation CTs showed low density of the irradiated portion of liver, sharply demarcated from the liver outside of the radiation ports. On follow-up CT scans between 4 and 14 months after radiation therapy, the low-density band had resolved and liver function was returned to normal unless affected by progression of the primary cancer (Jeffrey et al. 1980).

Unger et al. later described the CT and MR imaging findings of two cases reports of RILD (Unger et al. 1987). This group confirmed the CT findings of low attenuation in the portion of irradiated liver, again sharply demarcated from unirradiated liver. This area of low density could represent increased water or fat content. An MR of the same patients showed decreased signal intensity on T1-weighted images, increased signal intensity on T2-weighted images, and increased signal intensity on proton spectroscopic imaging in the portion of liver corresponding to the low attenuation on CT, indicating that the irradiated liver consisted of increased water content. On follow-up CTs, there was resolution of the low attenuation portion of liver, and shrinkage of the irradiated liver segment (Unger et al. 1987).

As seen above, CT and MR imaging provides anatomical data in RILD. Unger et al. also performed CT angiography on one patient and found that the liver in the radiation ports demonstrated delayed filling of contrast as compared to unirradiated liver, alluding to the outflow congestion pattern found on pathology (Unger et al. 1987). This was the first step toward identifying the perfusion changes of the liver as it relates to RILD.

Noninvasive CT imaging and the estimation of blood flow by the gradient method was first described for the kidney (Peters et al. 1987a, b). The quantification of blood flow was later described in a mathematical model using information obtained from dynamic CT and read on a color scale (Miles 1991; Miles et al. 1991). Although some groups have used the gradient method to measure liver perfusion (Miles et al. 1993; Blomley et al. 1995; Bader et al. 1998), the liver poses a unique challenge given that it has dual vascular input from the hepatic artery and the portal vein. Materne et al. first developed and validated a method to quantify liver perfusion using the "dual-input, one-compartment" model to account for the dual inflow (Materne et al. 2000).

The finding of VOD in RILD implies that the vascular outflow will be altered, namely in a post-hepatic obstruction manner beginning at the level of the central veins and further distally to the hepatic veins. CT perfusion is an imaging technique that can identify and quantify this vascular flow aberrancy (Cao et al. 2008).

MR single-photon emission computerized tomography (SPECT) has been used to measure asialoglycoprotein receptor (ASGPR). ASGPRs are receptors found in abundance on the sinusoidal surface of hepatocytes that mediate the removal of serum glycoproteins, lipoproteins, immunoglobulin A, fibronectin, and apoptotic cells. They, therefore, can serve as a surrogate for hepatic function. Iguchi et al. (2003) have shown that ASGPR SPECT correlates well with liver fibrosis (Hoefs et al. 2006).

Table 3 SOMA grading system for liver injury

Liver				
	Grade 1	Grade 2	Grade 3	Grade 4
Subjective				
Pain RUQ	Occasional and minimal	Intermittent and tolerable	Peristent and intense	Refractory and excruciating
Objective				
Abdominal findings Edema Weight gain Alertness Bleeding	Hepatomegaly Occasional leg edema	Soft ascites Intermittent leg edema ≤5 % Change in attentiveness and sleep pattern	Tense ascites Anasarca responsive to diuretics >5–10 % Confusion Correctable	Anasarca unresponsive to diuretics >10 % Coma Unresponsive
Management				
Pain Abdominal findings Bleeding	Occasional non-narcotic	Regular non-narcotic Intermittent diuretics Iron therapy	Regular narcotic Permanent diuretics Occasional transfusion of fresh frozen plasma	Continuous narcotic Frequent transfusions
Analytic				
AST/ALT/Alk phos	<2.5 × normal	2.5–5.0 × normal	>5.0–20.0 × normal	>20.0 × normal
Bilirubin	<1.5 × normal	1.5–5.0 × normal	>5.0–10.0 × normal	>10.0 × normal
PT/PTT	<1.25 × normal	1.25–1.5 × normal	>1.50–2.0 × normal	>2.0 × normal
Serum alb (gm/dl)[3]	>3.0	>2.5–3.0	>2.0–2.5	≤2.0
Platelets (1,000)	>75.0	>50.0–75.0	>25.0–50.0	≤25.0

5 Radiation Tolerance and Predicting Liver Toxicity

5.1 Clinical Parameters

Pre-existing liver dysfunction makes patients more susceptible to radiation-induced liver injury, as summarized in Table 3. Patients with Child-Pugh B or C scores have a higher risk of radiation-associated liver toxicity than those with Child-Pugh A scores (Liang et al. 2006; Hata et al. 2006; Ten Haken et al. 2006). Additional risk factors include hepatitis B carrier status (Cheng et al. 2004a), prior transarterial chemoembolization (TACE) (Liang et al. 2006), concurrent chemotherapy (Dawson et al. 2002), portal vein tumor thrombosis (Kim et al. 2007; Liang et al. 2006; Seong et al. 2003), tumor stage (Liang et al. 2006), male sex (Dawson et al. 2002), and cancer of the liver Italian program (CLIP) staging system (Liang et al. 2006; Seong et al. 2003, 2007).

As a measure of baseline liver reserve, baseline indocyanine green retention rate at 15 min was investigated and found to correlate with hepatic insufficiency following proton ion therapy for 30 patients with hepatocellular carcinoma (Kawashima et al. 2005). Eight patients developed hepatic insufficiency, presenting as anicteric ascites, elevated transaminases and/or asterixis, 1–4 months following therapy. No hepatic insufficiency was observed if the retention rate was less than 20 %, whereas 3 of 4 patients with retention rates greater than 50 % developed hepatic insufficiency.

The tolerance of the liver to whole organ irradiation does not appear to be substantially altered by the concomitant use of fluoropyrimidines. In contrast, whole liver irradiation in combination with alkylating agents or mitomycin C is associated with an increased risk of liver toxicity (Lawrence et al. 1995; Haddad et al. 1983; Schacter et al. 1986). In one study investigating the partial volume tolerance of the liver to irradiation, the use of concurrent hepatic arterial bromodeoxyuridine (BUdR) chemotherapy increased the risk of RILD compared to concurrent hepatic arterial fluorodeoxyuridine (FUdR) (Dawson et al. 2002).

5.2 Dosimetric Parameters

5.2.1 Whole Liver Tolerance

The classic paper by Ingold et al. published in 1965 is the first report of a dose-complication relationship for whole liver irradiation (Ingold et al. 1965). RILD occurred in 1 of 8 patients who received 30–35 Gy over 3–4 weeks and 12 of 27 patients who received 35 Gy or more to their whole liver. Since then, many clinical series have been published supporting that the whole liver tolerance to radiation of

30–35 Gy in 2 Gy per fraction associated with a 5 % risk of RILD. In 1973, whole liver doses of 2.25 Gy × 8 fractions were reported to be safe, but 3.5 Gy × 8 was associated with a high rate (8/25) of liver toxicity (Wharton et al. 1973; Perez et al. 1978), showing the importance of fraction size. An apparent lower whole liver threshold was seen in patients treated with the 'moving strip technique', where RILD was observed following 22–25 Gy delivered to the whole liver (Schacter et al. 1986). However, there is much uncertainty of the actual doses delivered using the 'moving strip techniques', and the delivered doses were likely higher than the planned whole liver doses. In the 1991 report by Emami et al., the TD 5/5 for whole liver radiation was estimated to be 30 Gy in 2 Gy fractions (Emami et al. 1991).

Hyperfractionation was investigated as a strategy to reduce toxicity, but the tolerance to whole liver irradiation did not improve substantially. In a Radiation Therapy Oncology Group (RTOG 8405) dose escalation study of accelerated hyperfractionation, none of the 122 patients who received 27–30 Gy in 1.5 Gy fractions twice daily to the whole liver experienced RILD, whereas 5 of 51 who received 33 Gy in 1.5 Gy fractions developed RILD (Russell et al. 1993).

Another study (RTOG 7609) investigated whole liver radiation therapy for palliation of 103 patients with liver metastases. The fractionation schedules (and number of patients) were 26 Gy in 16 fractions (n = 38), 30 Gy in 10 (n = 19), 15 (n = 2), or 19 (n = 5) fractions, 20 Gy in 10 fractions (n = 19), or 21 Gy in 7 fractions (n = 18). Although no RILD was reported, the median survival was 11 weeks, and approximately 23 % of patients did not complete their planned treatment. Progressive disease may have masked RILD or led to early death before RILD could manifest, limiting a detailed interpretation of these data. As 17 of the 18 patients treated with 21 Gy in 7 fractions completed treatment as planned, this regimen has been recommended as the fractionation of choice of those studied (Borgelt et al. 1981).

More recent experience has suggested that the whole liver doses associated with a 5 % risk of classic RILD are 32 and 37 Gy in 1.5 Gy twice daily for patients with primary liver cancer and metastases, respectively (Dawson et al. 2002). In 2 Gy per fraction, the mean liver doses estimated to be associated with a 5 % risk of classic RILD for primary and metastatic liver cancer are 28 and 32 Gy.

5.2.2 Partial Liver Tolerance

In 1965, Ingold et al. safely delivered 55 Gy to parts of the liver (Ingold et al. 1965). The first quantitative analysis of RILD as a function of dose and volume was performed by Austin Seymour et al. in 1986. Dosevolume histograms (DVHs) from 11 patients treated with charged particles for pancreatic or biliary cancer (one of whom developed liver toxicity) were reviewed. Patients were treated with a total dose of 52–70 Gy. It was concluded that doses in excess of 35 Gy should be limited to 30 % of the liver when 18 Gy was delivered to the whole liver (equivalent to photon 2 Gy/day).

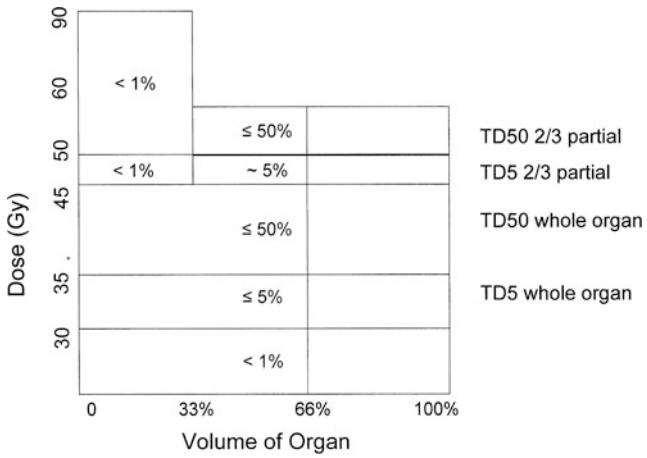

Fig. 8 Dose–volume histogram for liver toxicity, illustrating the relationship between volume and tolerance doses, assuming uniform partial volume irradiation

In 1991, Emami et al. reported estimates of the tolerance doses for 5 % and 50 % risk of liver toxicity (TD 5/5 and TD 50/5 respectively) following uniform liver RT (Emami et al. 1991). For one-third, two-thirds, and the whole liver tolerances, the estimated TD 5/5 were 50 Gy, 35 Gy, and 30 Gy, respectively, (at 1.8–2 Gy/day) and the estimated TD 50/5 were 55, 45, and 40 Gy, respectively (at 1.8–2 Gy/day) (Emami et al. 1991). These estimates were based primarily on clinical judgment from retrospective reports of suspected radiation injury in less than 30 patients, as detailed partial dose and volume data were not generally available at the time of this report.

Since Emami's review, there has been many published reports of patients treated with partial liver irradiation using photons (Cheng et al. 2003; Liang et al. 2006; Ten Haken et al. 2006; Dawson et al. 2002, 2005), protons (Hata et al. 2006; Chiba et al. 2005; Ohara et al. 1997), and hypofractionated stereotactic body radiotherapy (SBRT) (Herfarth et al. 2001, 2004; Uematsu et al. 2000). Clinically significant liver toxicity is not common following focal proton therapy (Hata et al. 2006; Chiba et al. 2005; Ohara et al. 1997) or SBRT (discussed in Sect. 5.4). Figure 8 summarizes the whole and uniform partial volume tolerances of the liver.

The largest series of patients treated with partial liver radiation therapy is from the University of Michigan (Dawson et al. 2002). Dose was prescribed based on the DVH of the normal liver (the effective volume (V_{eff}) of

Table 4 Series of fractionated partial liver irradiation and rates of RILD from Pan et al. (2008), with permission

Study group	N	Diagnosis	Baseline Child-Pugh score	Prescription dose fractionation	Crude percent RILD	Mean normal liver dose in patients with versus without RILD	Factors associated with RILD
Michigan (Dawson et al. 2002; Dawson and Ten Haken 2005)	203[a]	PLC + LMC	203 A	1.5 Gy bid	9.4 % (19/203)	37 Gy versus 31.3 Gy	PLC versus LMC Mean liver dose
Taipei (Cheng et al. 2004b)	89[b]	HCC	68 A 21 B	1.8–3.0 Gy	19 % (17/89)	23 Gy versus 19 Gy	HBV, liver cirrhosis
Shanghai (Xu et al. 2006; Liang et al. 2006)	109[b]	PLC	93 A 16 B	4–6 Gy	15.6 % (17/109)	24.9 Gy versus 19.9 Gy	Liver cirrhosis
Guangdong (Wu et al. 2004)	94 [b]	HCC	43 A 51 B	4–8 Gy	17 % (16/94) Note: 4 fatal	Not stated	Liver cirrhosis
S Korea (Seong, Park) (Park et al. 2002; Seong et al. 2003)	158[b]	HCC	117 A 41 B	1.8 Gy	7 % (11/158)	Not stated	Dose
S Korea (Kim) (Kim et al. 2007)	105[b]	HCC	85 A 20 B	2.0 Gy	12.3 % (13/105)	25.4 Gy versus 19.1 Gy	Total liver volume receiving 30 Gy or more above 60 %

[a] Patients also received FUdR or BUdR; in this series, the mean normal liver dose was calculated as corrected for 1.5 Gy bid equivalent dose, and the comparison of patients with versus without RILD refers to the median value of mean normal liver dose, whereas for other series the comparison is between the average (mean) of mean normal liver dose in each group

[b] At least 77 % of patients in these series also received trans-arterial chemoembolization (TACE)

HCC hepatocellular carcinoma; *PLC* primary liver cancer; *HBV* hepatitis B viral infection

normal liver irradiated) and patients were prospectively followed for RILD (Ten Haken et al. 1993). The 203 patients with primary and metastatic liver cancer were treated with 3D conformal radiation therapy delivered concurrently with hepatic arterial chemotherapy (FUdR or BUdR). All patients had Child-Pugh A liver scores. This experience demonstrated that small portions of the liver can be irradiated to very high doses (up to 90 Gy in 1.5 Gy twice daily), and that mean liver dose is strongly associated with risk of RILD (as discussed in Sect. 5.2.3.2).

Cheng et al. reported on liver toxicity that developed in 17 of 89 patients with hepatocellular carcinoma treated with focal photon RT and TACE (Cheng et al. 2005). The majority of these patients had a diagnosis of hepatitis B (73 %) and hepatitis C (21 %), and 24 % had Child-Pugh B scores at baseline. The majority of the complications were non-classic RILD (elevated serum transaminases, 15 patients) versus classic RILD (2 patients). Multivariate analysis revealed that hepatitis B virus and Child-Pugh liver score were independently associated with increased risk of liver toxicity. In all patient subgroups, the tolerance of the liver to radiation was lower than that reported from the University of Michigan, perhaps due to the sequential use of TACE which may have decreased the liver reserve and the patient population which included patients with hepatitis B and poor liver function (Child-Pugh B).

Table 4 includes series in which toxicity has been described and quantified after partial liver irradiation. In most, the key factor predicting RILD was the baseline condition of the liver, but dosimetric parameters (e.g. mean liver dose and volume receiving 30 Gy or more (V30)) were also associated with increased toxicity risk. In each series, where mean normal liver dose was reported for patients with or without RILD, the mean dose for patients with RILD was higher (Pan et al. 2008). V30 has been studied mostly in hepatocellular carcinoma patients, with both classic and nonclassic RILD endpoints combined. V30 segregates higher risk patients from lower risk patients in some studies at cutoff levels of 28–60 % (Kim et al. 2007; Liang et al. 2006; Yamada et al. 2003); however, the effect of V30 is not uniformly observed (Cheng et al. 2002). Other studies suggest the importance of V20–V40 (Kim et al. 2007) and V5–V40 (Liang et al. 2006), but only for Child-Pugh A patients in the latter study.

5.2.3 Normal Tissue Complication Probability Models

5.2.3.1 Lyman NTCP Model

The Lyman normal tissue complication probability (NTCP) model has been used to describe the volume dependence of RT normal tissue toxicity (Lyman 1985). It assumes a

sigmoid relationship between the dose of uniform radiation given to a volume of an organ and the chance of a complication occurring. The Lyman model uses three parameters: $TD_{50}(1)$, the whole liver dose associated with a 50 % probability of toxicity, 'm', characterizing the steepness of the dose–response at $TD_{50}(1)$, and 'n', a volume effect parameter which indicates a larger volume effect as it increases (range 0–1). The Lyman NTCP model was first applied to clinical data in 1991 by Burman et al. (1991), who used the estimated partial liver tolerances by Emami et al. to calculate the Lyman model parameters. The value of $TD_{50}(1)$, 'm', and 'n' were 45 Gy, 0.15, and 0.32, respectively.

In 1992, Lawrence et al. analyzed the DVHs of 79 patients with hepatic malignancies (9 with RILD) using the Lyman NTCP model with the KB Veff DVH reduction scheme (Lawrence et al. 1992). The $TD_{50}(1)$ and 'm' parameters were similar to the previous estimates; however, a larger volume effect parameter ($n = 0.69$) was found. More recently, data from 204 patients (19 with classic RILD) were evaluated using the Lyman model (Dawson et al. 2002). The volume effect parameter was again higher than previously estimated, with a value of 0.97.

In addition to dosimetric factors, the influence of clinical and demographic factors on the development of classic RILD in these 203 patients were investigated using a multivariate analysis (Dawson et al. 2002). Mean liver dose ($p < 0.0001$), primary hepatobiliary carcinoma diagnosis ($p = 0.005$), BUdR chemotherapy ($p < 0.0001$), and male sex (0.002) were statistically significant factors associated with RILD. Lyman NTCP model parameters were then fit for subgroups that were predicted to have different risks of RILD. In 169 patients treated with FUdR, 'n' and 'm' were fit to the entire group, but $TD_{50}(1)$ was separately fit for patients with primary liver cancer ($TD_{50}(1)_{HB}$) (n = 84) and liver metastases ($TD_{50}(1)_{LM}$) ($n = 85$). The parameters and 95 % CI's were as follows: 'n': 0.97 (0.69, 2.3), 'm': 0.12 (0.07, 0.25), and $TD_{50}(1)_{HB}$: 39.8 Gy (38.8, 41.1) and $TD_{50}(1)_{LM}$: 45.8 Gy (43.4, 50.4), ($D = 66.0$, $p > 0.99$), indicating a higher tolerance of the liver to radiation for patients with liver metastases compared to primary hepatobiliary malignancies and a strong correlation of RILD risk with the mean liver dose. The tolerance doses for one-third and two-thirds uniform partial liver irradiation associated with a 5 % risk of RILD are >100 and 54 Gy, respectively, for metastases, and 93 and 47 Gy, respectively, for primary liver cancer (in 1.5 Gy bid) (Dawson et al. 2002).

The Lyman NTCP model has also been used to estimate partial liver tolerance to irradiation in patients with hepatocellular caricinoma irradiated in Asia. In the Taiwanese (Cheng et al. 2003) and Chinese (Liang et al. 2006; Ten Haken et al. 2006) series (including mostly hepatitis B patients), the tolerance of the liver to radiation was less predictable. The most common toxicity was elevation of transaminases rather than classic RILD. In the Taiwanese series of RILD (15 nonclassic, 2 classic) in 17 of 89 patients with hepatocellular carcinoma treated with focal photon RT and TACE (Cheng et al. 2005), 'n' was low ($n = 0.26$) in patients with hepatitis B, and closer to 1 ($n = 0.86$) in nonhepatitis B patients. The tolerance of the liver to radiation was lower than that reported from the University of Michigan. In other Asian studies, both classic and nonclassic RILD were also included as toxicity endpoints. The range of estimates of the parameters generated among patients with Child-Pugh A or better liver function and no hepatitis B virus (HBV) infection are as follows: n, 0.86–1.1; m, 0.12–0.31; and TD_{50}, 39.8–46.1 Gy. For patients with HBV or Child-Pugh B liver dysfunction, the ranges are as follows: n, 0.26–0.7, m, 0.4–0.43, and TD_{50}, 23–50 Gy, demonstrating a lower tolerance to irradiation in these patients. In some of these series, larger fraction sizes were used, which may have also contributed to the differences in TD_{50} values between these series and the Michigan experience (Ten Haken et al. 2006).

5.2.3.2 Mean Liver Dose Model

An 'n' of 1 in the Lyman NTCP model suggests a large volume effect and a strong correlation of NTCP with mean liver dose. For patients studied in the University of Michigan experience, beyond a threshold mean liver dose of 30 Gy (below which no patient developed RILD), Lyman NTCP increased by approximately 4 % per Gy increase in mean dose. The mean liver dose associated with a 5 % risk of RILD for patients with metastatic and primary liver cancer are 37 and 32 Gy, respectively, in 1.5 Gy per fraction, and 32 and 28 Gy in 2 Gy per fraction, respectively, (assuming an α/β of 2 for the liver) (Fig. 9). The risk of classic RILD associated with different mean liver doses can be estimated by correcting for differences in dose per fraction.

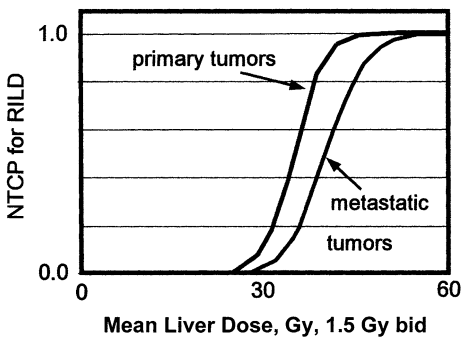

Fig. 9 Mean liver dose, corrected with LQ modeling for 1.5Gy per fraction, versus Lyman normal tissue complication probability (NTCP) of radiation-induced liver disease (RILD) for primary and metastatic liver cancer, redrawn from Dawson and Ten Haken (2005) with permission

5.2.3.3 Local Damage: Organ Injury NTCP Model

As the Lyman model is simply a sigmoid dose–response function, efforts have been made to develop models that will accommodate biological data when they are available. These "damage-injury" (D-I) models try to use statistical principles to derive the RT tolerance of an organ from dose–response characteristics of individual functional subunits. These models are most appropriate for organs with parallel architecture, such as the liver, where it is assumed that the organ functions (sustains damage) until a critical fraction of the organ becomes incapacitated (and injury occurs).

In 1995, Jackson et al. analyzed an extension of the University of Michigan's original dataset using a D-I NTCP model (Jackson et al. 1995). The model fits the data from 95 patients well; however, uncertainties in the functional reserve distribution and subunit radiosensitivity were highly correlated. The D-I model parameters were as follows: D_{50} (the dose associated with a 50 % probability of voxel or subvoxel damage) = 42 Gy; k (describing the steepness of the "local damage" function) = 1.95; F_{50} (the fraction of the total organ incapacitated which would produce a 50 % complication rate) = 0.497; and σ_v (describing the steepness of the "organ" response function) = 0.05. The partial liver volume threshold, below which the complication risk becomes near zero for all doses, was 0.4.

Data from more patients (203) were subsequently fit using the D-I NTCP model (Dawson and Ten Haken 2005), and the most substantial differences were in the F_{50} and σ_v parameters ($F_{50} = 0.4$, $\sigma_v = 0.08$), suggesting a lower threshold and a shallower slope for population cumulative functional reserve than previously estimated, predicting more complications for a lower fractional damage (Dawson et al. 2005). The revised RT volume threshold for complications was 0.25. Of note, the 68 % confidence intervals for the D-I NTCP model parameters are very large, and thus much more clinical data is required to validate the D-I NTCP model parameters. Nonetheless, such a model motivates the search for functional imaging that will measure functional subunit tolerance to irradiation.

In another analysis from the Taiwan group of patients with hepatocellular carcinoma and gastric cancer, valid fits were only obtained for the nonHBV carriers with local damage parameters of $D_{50} = 25$ Gy, $k = 60$; and fraction of liver injury required for RILD parameters of $F_{50} = 0.59$, $\sigma = 0.12$(Cheng et al. 2005).

5.2.3.4 Sensitivity of NTCP models

The largest uncertainty in NTCP model parameters is likely due to the model fitting, and relatively small number of events (i.e. complications), compared to the 3 or 4 parameters required to be fit. As values for some parameters can be measured or estimated with better certainty, the uncertainty of other NTCP model parameters will decrease and the utility of NTCP models will increase. Other geometric and dosimetric uncertainties can also impact the confidence intervals of NTCP parameter estimates.

The liver is relatively easy to identify on simulation CT scans. The magnitude of the errors introduced by including the biliary duct system and hepatic vasculature in the "liver volume" is unclear, though probably minimal, as most series likely contoured the liver in a similar manner. Of note, the liver minus the gross tumor volume was used for the Michigan analysis and most others. NTCP values may differ if another liver volume is used for analysis of NTCP.

Liver motion due to breathing has been shown to alter the delivered radiation doses. The technique used to deliver irradiation also influences the uncertainty in delivered doses with larger uncertainties, with older techniques such as the moving strip technique, and also with more modern techniques of intensity modulated radiation therapy in the absence of image guidance.

Changes in dose per fraction may also alter NTCP model parameters, compared to the fractionation in which they were obtained.

5.3 Intensity Modulated Radiation Therapy

Few papers on liver tolerance have focused on intensity modulated radiation therapy (IMRT), and the effects of different spatial dose distributions are not well established. IMRT lead to a low dose 'bath' delivered to a larger volume compared with simpler plans which usually completely spare RT to a portion of the liver. This bath of low dose may impact the partial tolerance of the liver to RT, and it may reduce the possibility for a compensatory increase in function. For the same mean dose to the liver, a bath of low dose to a larger volume has been hypothesized to be associated with a higher risk of RILD compared to higher doses delivered to a smaller volume, based on an analysis of the Michigan data using principal component analysis (Dawson et al. 2005).

5.4 Stereotactic Body Radiation Therapy

RILD is uncommon following SBRT for liver metastases, but has occasionally been reported (Blomgren et al. 1995; Hoyer et al. 2006; Mendez et al. 2006). In order to keep the risk of liver toxicity low, a substantial volume of liver must be spared from irradiation. This can be done by keeping the dose to 700 cc of uninvolved liver less than 15 Gy in three fractions (Kavanagh et al. 2006) or ensuring that no more than 50 % of the liver receives 15 Gy in 3 fractions (or 7 Gy in one fraction), and no more than 30 % of the liver receives 21 Gy in 3 fractions (or 12 Gy in one fraction) (Herfarth et al. 2004).

Mendez-Romero et al. observed 1 classic and 1 non-classic case of RILD among 8 patients with hepatocellular carcinoma (HCC) treated on a trial of SBRT for liver tumors; another patient with baseline Child-Pugh B liver dysfunction and HCC experienced portal hypertension and concomitant nonhepatic infection and died 2 weeks after treatment. No grade 4 or 5 toxicity occurred among the 17 patients with liver metastases treated on the trial, consistent with the finding that hepatocellular carcinoma patients are more susceptible to liver toxicity (Mendez et al. 2006). In a phase II study involving 61 patients treated with 3 fraction SBRT for colorectal metastases, Hoyer et al. observed liver toxicity in 1 patient following SBRT. In this case, 60 % of the liver received 10 Gy or higher, with a median dose of 14.4 Gy. This patient died of hepatic failure 7 weeks after treatment, but the authors could not prove that the cause was radiation-induced liver toxicity (Hoyer et al. 2006). In a Princess Margaret Hospital study of patients treated with 6 fraction SBRT for hepatocellular caricnoma or intrahepatic cholangiocarcinoma, 17 % patients experienced progression from Child-Pugh A to B within 3 months after treatment (Tse et al. 2008), although this was more common in patients irradiated to low doses, with intrahepatic cancer progression.

In the University of Colorado trial of SBRT for liver metastases, a modification of a critical volume model (Yaes and Kalend 1988) was applied to attempt to avoid liver toxicity. A minimum "critical volume" required to be spared from radiation therapy was estimated from surgical series to be 700 cc. The maximum dose allowed to the critical volume was 15 Gy in 3 fractions (Schefter et al. 2005). No RILD or other severe toxicity has been observed after SBRT for 18 patients with liver metastases (Schefter et al. 2005). The median mean liver dose (to liver minus the tumor volume) in patients treated was 15.3 Gy (3.3–23.9 Gy), in 3 fractions. Figure 10 displays the mean DVH from the first 18 patients treated with SBRT in Colorado, without toxicity.

A potential concern related to the use of high dose per fraction treatment is the observation of extrahepatic portal vein occlusion following high-dose intraoperative radiation therapy (IORT). Mitsunaga and colleagues observed this in 12 of 53 patients who underwent pancreaticoduodenectomy for periampullary disease followed by 20 Gy IORT to the resection bed (Anscher et al. 1993).

5.5 Compensatory Response

Following partial liver irradiation, shrinkage of the high-dose irradiated volume is seen on follow-up CT and MR imaging. A compensatory increase in liver volume in the unirradiated regions is also commonly seen, as shown in Fig. 7 (Herfarth et al. 2003; Ohara et al. 1997).

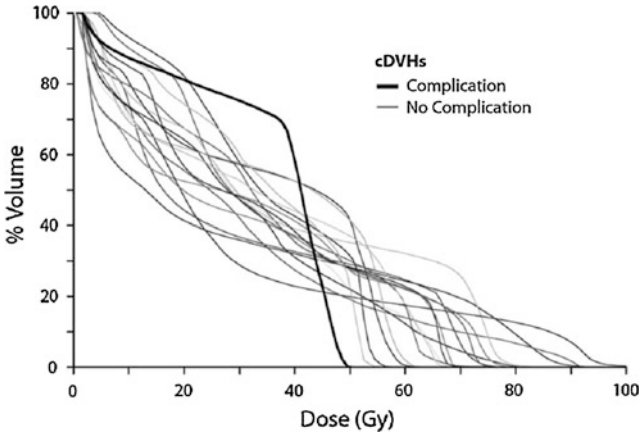

Fig. 10 All cumulative partial liver (minus GTV) cumulative dose–volume histograms (cDVHs) with Lyman NTCP of 1%. The cDVH associated with complication is shown in bold. This cDVH had a larger dose to a smaller volume, compared to the other cDVHs with a larger volume treated to a higher dose, from Dawson et al. (2005), with permission

5.6 Recommended Dose/Volume Constraints

Recommendations for dose/volume constraints are outlined in Table 5. These dose/volume recommendations are associated with some uncertainty and they will vary depending on the technique used, concurrent therapies, and patient population investigated.

6 Chemotherapy

Many chemotherapy agents have the potential for producing liver damage. Determining the cause of abnormal liver function tests developing during chemotherapy can be complex and may relate to pre-existing liver dysfunction, reactivation of a dormant virus, or directly related to hepatic toxic drugs. The cause of liver toxicity in patients with liver metastases or liver cancer can also be challenging, as progressive disease or systemic symptoms of metastatic disease, such as nutritional deficiencies, may be responsible. Therefore, baseline evaluation of patients' prechemotherapy should include liver function tests and typically a CT scan or ultrasound (U/S) which are usually done as part of staging. This assessment of liver function before chemotherapy aids in the choice of drug and dose. Repeat evaluation of liver function during therapy can detect the evolution of hepatic dysfunction and help determine if progressive disease is partially responsible. These tests can also help determine the need for dose modification during treatment.

The following overview outlines the different patterns of liver toxicity and their manifestations. Table 6 outlines some of the most common chemotherapy-related liver toxicities. For a more extensive review, we refer the reader

Table 5 Suggested dose–volume constraints, from (Pan et al. 2008) and Quantec

Palliative whole liver doses for 5 % or less risk of RILD
Liver metastases
≤30 Gy, in 2 Gy per fraction
21 Gy in 7 fractions (Borgelt et al. 1981)
Primary liver cancers
≤28 Gy, in 2 Gy per fraction
21 Gy in 7 fractions (Abrams et al. 1997)
Therapeutic partial liver radiotherapy (standard fractionation)
Mean normal liver dose (liver minus GTV)
<28 Gy in 2 Gy fractions for primary liver cancer
<32 Gy in 2 Gy fractions for liver metastases
Nonuniform liver recommendations (SBRT, 3–6 fractions)
Mean normal liver dose (liver minus GTV)
<13–20 Gy for primary liver cancer
<15–22 Gy for liver metastases
Critical volume model-based
≥700 cc of normal liver receives ≤ 15 Gy in 3–5 fractions (Schefter et al. 2005)

to references focusing on chemotherapy-related toxicities (Davila and Bresalier 2008; King and Perry 2001).

6.1 Mechanisms of Toxicity

- *Toxic hepatitis*. This form of hepatic injury is usually due to a direct effect of either the parent drug or a metabolite and the pattern of injury is predictable. It typically manifests as elevations of hepatic enzymes preceding increases in total bilirubin as cellular damage occurs. As the toxic effect progresses, fatty infiltration and cholestasis may occur with severe toxicity resulting in hepatocellular necrosis.
- *Idiosyncratic reactions*. Most toxicity is idiosyncratic and thought to be due to host response and possibly immunologic mechanisms. This form of toxicity is unpredictable, not dose-dependent, and can occur with nearly every drug in clinical use. There is no relationship between the drug dose and the occurrence of the drug reaction. Rechallenge with the offending agent is not recommended as there is usually a recurrence of symptoms, particularly if the reaction was immunologically based.

6.2 Patterns of Drug-Induced Liver Injury

Acute drug-induced liver may present as hepatocellular damage, cholestasis, fibrosis, or steatosis. The presentations range from asymptomatic, mild biochemical abnormalities to an acute illness with jaundice that resembles viral hepatitis to acute liver failure. Withdrawal of the offending drug usually leads to reversal of the injury. However, some types of toxicity can be associated with a progressive course, possibly leading to fibrosis or cirrhosis, despite discontinuation of the drug. Other drugs can cause endothelial damage or thrombosis leading to vascular complications such as sinusoidal obstructive syndrome (SOS).

- *Hepatitis*. Drug-induced acute hepatocellular injury is similar to that seen in viral hepatitis and includes hepatocellular necrosis, steatosis, and cellular degeneration. A characteristic finding on laboratory testing is an elevation in serum aminotransferases. Acute hepatocellular injury is associated with a mortality rate of up to 10 % overall and up to 80 % or higher if acute liver failure develops (Ostapowicz et al. 2002; Speeg and Bay 1995). A serum bilirubin >3 times the upper limit of normal is the best predictor of mortality in the setting of acute hepatocellular injury (Bjornsson 2006).
- *Cholestasis*. Cholestatic reactions are typically associated with elevated alkaline phosphatase and bilirubin levels with a lower rise in aminotransferases. Gemcitabine, a fluorine analogue, has broad antitumor activity and is used in the treatment of a variety of cancers. It frequently causes transient, reversible elevations in transaminases although there are reports of fatal cholestatic hepatotoxicity (Coeman et al. 2000; Robinson et al. 2003). Pre-existing liver metastases and/or bilirubin level higher than 1.6 mg/dL at treatment onset are risk factors for developing liver failure (Rodriguez-Frias and Lee 2007; Sessa et al. 1994).
- *Steatosis/steatohepatitis*. Nonalcoholic fatty liver disease ranges in severity from nonprogressive steatosis to steatohepatitis, characterized by inflammation and hepatocyte injury that can progress to cirrhosis and fibrosis. Although a causative association is unproven, radiographic evidence of steatosis is seen in 30–47 % of patients treated with fluorouracil (Zorzi et al. 2007). The association between irinotecan and steatohepatitis has been confirmed in a number of studies (Zorzi et al. 2007; Vauthey et al. 2006; Pawlik et al. 2007). This has important implications particularly when these agents are given in the neoadjuvant setting prior to resection for hepatic metastases related to colorectal cancer. Steatohepatitis is a contraindication to major liver resection and irinotecan should be avoided in patients with known steatosis or steatohepatitis in whom major hepatic resection is planned. To prevent adverse outcomes from chemotherapy-associated liver injury, extended preoperative chemotherapy should be avoided and several studies indicate that a longer interval between chemotherapy and hepatic resection reduces hepatotoxicity and surgical

Table 6 Summary of chemotherapy-associated liver toxicities

Agents	Toxicity	Frequency	Comments
Nitrogen mustards			
Chlorambucil	Fibrosis and cirrhosis	Rare	Severe damage reported
Cyclophosphamide	VOD in high doses or transplantation	10–25 % of BMT patients	Severe and life threatening
Ifosfamide	↑ Transaminases and bilirubin	Uncommon	Dose reduce with significant dysfunction
Melphalan	VOD, hepatitis, and jaundice ↑ Transaminases	VOD 10–25 % of BMT patients. Common at high doses	May be severe Usually transient
Nitrosoureas			
Carmustine	↑ Transaminases, ALP, and bilirubin	20–25 % of patients	Usually mild and reversible
Lomustine	↑ Transaminases, ALP, and bilirubin	Common	Usually mild and reversible
Streptozocin	Raised LFTs	Common (15–67 % of patients)	Usually asymptomatic and reversible
Platinum agents			
Carboplatin	↑ ALP, transaminases	Common	Transient
Cisplatin	↑ Transaminases Steatosis and cholestasis	Common at high doses Rare	Transient
Oxaliplatin	↑ Transaminases and bilirubin Sinusoidal obstruction syndrome and perisinusoidal fibrosis	Common Rare. Usually with combination therapy	SOS may increase morbidity after liver resection
Other alkylating agents			
Dacarbazine	Hepatic vein occlusion	Rare	Usually with combination chemotherapy
Busulfan	VOD in high doses Cholestatic hepatitis	Common in BMT (10–25 %) Rare	Prior XRT, chemotherapy, and stem cell transplant increase the risk of VOD
Folate analog			
Methotrexate	Cirrhosis and portal fibrosis ↑ Transaminases	More common with chronic use More common with high dose	Potentially irreversible Transient
Antimetabolites			
Fludarabine	Abnormal LFTs, liver failure	Rare	
Mercaptopurine	Intrahepatic cholestasis and focal centrilobular necrosis ↑ Transaminases, ALP, and bilirubin	Common at doses > 2.5 mg/kg/day	Dose reduce in patients with hepatic dysfunction
Capecitabine	Hyperbilirubinemia Hepatic failure, hepatic fibrosis, and hepatitis	Common—up to 25 % of patients Rare	
Cytarabine	↑ Transaminases (acute) VOD Hyperbilirubinemia, liver abscess, liver damage, and necrotizing colitis	Common Uncommon Rare	Reversible With high doses
Gemcitabine	↑ Transaminases Cholestatic hepatotoxic reactions	Common (up to 60 %) Rare	Usually transient and reversible Can be fatal
Antitumor antibiotics			
Bleomycin	Hepatotoxicity	Rare	
Doxorubicin	↑ Transaminases and bilirubin	Rare	Toxicity increased with hepatic dysfunction
Epirubicin	↑ Transaminases	Rare	Dose ↓ with mild/moderate hepatic dysfxn
Mitoxantrone	↑ ALP, transaminases, and γGT	> 10 %	Dose decrease with hepatic dysfunction
Dacarbazine	Fulminant hepatic failure	Rare	Can be life threatening

(continued)

Table 6 (continued)

Agents	Toxicity	Frequency	Comments
Other agents			
Etoposide	VOD in high doses Hepatitis	10–25 % of BMT patients Rare	Severe
Docetaxel	↑ Transaminases, bilirubin, and ALP	≥ 10 %	dose decrease in pts with hepatic dysfunction
Paclitaxel	↑ Transaminases, bilirubin, and ALP	≤37 % patients with high doses	Dose ↓ in patients with hepatic dysfunction
Vinorelbine	↑Transaminases and bilirubin	Common	Dose ↓ in patients with hepatic dysfunction
Irinotecan	Steatosis and steatohepatitis ↑Transaminases and bilirubin	Up to 50 % patients Up to 25 % patients	May ↑morbidity after liver resection Usually reversible
Topotecan	↑Transaminases and ALP	Uncommon	Reversible

VOD veno-occlusive disease, *BMT* bone marrow transplant, *ALP* alkaline phosphatase, *LFTs* liver function tests, *XRT* radiation therapy, *γGT* gamma glutamyltransferase

complications for patients with colorectal liver metastases (Kopetz and Vauthey 2008; Welsh et al. 2007). Tamoxifen, a selective estrogen receptor modulator, used in the treatment of estrogen receptor-positive breast cancer is associated with steatosis, reported in up to 30 % of cases and is associated with a two-fold increased risk of developing steatohepatitis, especially in overweight women (Bruno et al. 2005; Ogawa et al. 1998).

- *Sinusoidal obstruction syndrome* (*SOS*). Sinusoidal Obstruction Syndrome (SOS), described in Sect. 3.3.2, results from blockage of venous outflow in the small centrilobular and sublobular hepatic vessels and manifests clinically as marked elevations in serum enzymes and bilirubin, ascites, painful hepatomegaly, and weight gain from fluid retention. Hepatic SOS is one of the most serious and life-threatening toxicities of hematopoietic stem cell transplantation, with the highest risk in patients treated with high-dose cyclophosphamide with or without busulfan. The frequency of SOS after allogeneic transplantation varies, but is estimated to be 10–25 %. Pre-existing liver disease or previous liver irradiation might increase susceptibility and the radiation dose has been suggested to increase the risk of SOS, although it also occurs frequently without radiation therapy conditioning. Treatment is mainly supportive. Sinusoidal injury has been reported with oxaliplatin, with an incidence of 19–52 % in patients receiving preoperative oxaliplatin for colorectal liver metastases, although this does not appear to be associated with increased morbidity or mortality (Vauthey et al. 2006; Pawlik et al. 2007; Klinger et al. 2009).
- *Viral hepatitis*. Similar to irradiation, hepatic toxic drugs can cause reactivation of hepatitis B virus, possibly due to an increase in viral synthesis when the patient is immunosuppressed, followed by a rebound in the host immune response to infection when therapy is discontinued. Risk factors for hepatitis B reactivation include detectable hepatitis B virus DNA prior to chemotherapy, male sex, and use of steroids. This toxicity may occur with many chemotherapy regimens, including low-dose methotrexate. Prophylactic antiviral therapy (Lamivudine) appears to reduce the risk of reactivation. There is a less clear relationship between chemotherapy and hepatitis C reactivation. However, the presence of hepatitis C virus prior to chemotherapy does increase the risk of liver toxicity, likely due to the impaired liver reserve. No prophylaxis is established for Hepatitis C.

6.3 Targeted Molecular Agents

Monoclonal antibodies and tyrosine and nontyrosine kinase inhibitors are increasingly being utilized in the treatment of cancer. The common agents in use and their associations with hepatotoxicity are listed in Table 7 (Carlini et al. 2006; Ho et al. 2005; Saif 2008).

7 Special Topics

7.1 Pediatrics

There is no literature suggesting that the tolerance of the pediatric liver is less to radiation, despite the fact that many pediatric protocols recommend far lower doses to be delivered to the liver than in adult populations. This is partially due to the fact that many treatment strategies in pediatrics consist of combined chemotherapy and radiation therapy either in combination or in sequence, and that there are less studies of the tolerance of the pediatric liver to radiation, specifically the partial pediatric liver tolerance.

Table 7 Summary of molecular targeted agents and associated liver toxicities

Agents	Toxicity	Frequency	Comments
Gefitinib	Increased transaminases, ALP	Uncommon	Usually reversible
Erlotinib	Increased transaminases	1–10 %	Usually reversible
Sorafenib	↑ Transaminases, bilirubin	Uncommon	Not studied in severe hepatic dysfxn
Sunitinib	↑ Transaminases, ALP, and bilrubin	Common	Transient
Temsirolimus	↑ Transaminases, ALP	Common	avoid in severe hepatic dysfunction
Lapatinib	↑ Transaminases and bilirubin	Rare	May be severe
Imatinib	↑ Transaminases, ALP, and bilirubin Hepatic necrosis	Uncommon Rare	Usually after 1–3 months

Doses of 5–10 Gy in one fraction and 15–25 Gy over 2 weeks have been delivered to pediatric patients with hepatic hemangiomas, without development of RILD or other liver toxicities (Order and Donaldson 2003).

7.2 Radioisotope Therapy

Hepatic radiation injury due to interval deposits of radionuclides was first recognized with the use of thorium dioxide (Thorotrast), an alpha emitter used in the 1950s as a contrast medium for radiography of the liver, speen, and blood vessels in the 1940s. The mechanism is ingestion by Kupfer cells. Since $Thorium^{232}$ has a long half-life (1.4×10^{10} years), its persistent deposition decades later, can result in neoplastic transformation of the liver i.e. cholangiosarcomas, and hepatomas, cirrhosis (Rubin and Levitt 1964), and peliosis hepatitis, characterized by blood-filled cavities throughout the liver (Jirtle et al. 1990), hypothesized result from endothelial sinusoidal injury (Gushiken 2000) or hepatocyte necrosis.

The Therapeutic use of Au^{198} as a radiogold colloid was first utilized by Rubin in treating disseminated reticular endothelial cell neoplasm, prior to effective chemotherapy for Non-Hodgkin's Lymphoma. The rationale was when lymphomas infiltrate the liver, the cellular infiltrates diffuse and radiogold would be deposited in a parallel diffuse fashion in Kupfer cells of the liver. Patient treated had extreme hepatomegaly, splenomegaly, and bone marrow infiltration. He was hospitalized for bone marrow aplasia and recovered. The patient survived for decades. Kaplan subsequently developed a protocol to treat Stage III/IV Hodgkin's if the spleen was involved with disease, post splenectomy (Rubin and Levitt 1964), radiogold was administered intravenously to selectively eradicate microdeposits of Hodgkin's disease infiltrates (Rubin and Levitt 1964).

Since then, hepatic arterial delivery of radioisotopes (Welsh et al. 2006; Gray et al. 2001; Stubbs et al. 2001; Kennedy et al. 2006; Tian et al. 1996) has been used more extensively to treat primary and metastatic liver cancers. A variety of radioisotopes have been investigated, but Yttrium-90 (Y^{90}), tagged glass, or resin microspheres is what is commercially available and most commonly used. Y^{90} has an effective pathlength of 5.3 mm (i.e. 90 % of the energy is deposited within a 5.3 mm radius of the microsphere). A typical prescribed dose is 120–150 Gy, where the microspheres (and dose) are primarily deposited at the periphery of the tumor (Kennedy et al. 2004).

Classic and nonclassic liver toxicity have been observed following Y^{90} microsphere therapy, but they are not common, despite delivery of very high focal liver doses (Neff et al. 2008). The safe delivery of high dose Y^{90} to small volumes appear consistent with the partial volume estimates from conformal radiation and SBRT series, as the estimated effective liver volume irradiated following Y^{90} microsphere therapy, is small (<20 %), due to rapid dose fall off of dose around each microsphere.

In a review of toxicities in 121 patients treated with hepatic arterial Y^{90}, liver toxicity was the most common toxicity, seen in 14 patients. At baseline, portal vein thrombosis was present in 25 % of patients, ascites in 19, and 20 % of patients had a Child-Pugh score of B. Risk factors associated with 90 day mortality, a surrogate for serious acute toxicity, were evaluated. Seven variables were studied, including five liver reserve variables (infiltrative tumor, tumor volume greater than 70 % of liver, tumor volume greater than 50 % of liver and albumin ≤3 g/dL, bilirubin ≥2 mg/dL, AST/ALT ≥5 times upper limit of normal) and 2 nonliver reserve variables (lung dose >30 Gy, non HCC diagnosis). Ninety day mortality was 49 % in 33 'high risk' patients with at least one adverse variable and 7 % in 88 'low risk' patients with no adverse variables. Eleven of the 12 fatal treatment related toxicities were in the 'high risk' group, which predominantly included patients with poor underlying liver function (Goin et al. 2005). In the 99 'low risk' patients, the most frequent toxicities were ascites, elevated bilirubin, and elevated transaminases, which were mostly transient. Elevated pretreatment bilirubin level and radiation dose were significantly associated liver toxicity in the 'low risk' patients ($p = 0.001$ and $p = 0.08$ respectively). Furthermore, shorter time between treatments in 23 patients who had two or more Y^{90} courses was

associated with an increased risk of liver toxicity ($p = 0.05$) (Goin et al. 2005). The lack of a validated dose distribution in Y^{90} treatment makes partial liver tolerance analysis challenging for Y^{90} therapy.

Intravenous radiolabeled monoclonal antibodies, antibody fragments, and low molecular weight peptides, can also cause liver toxicity, if radioisotopes deposit dose locally within the liver. Liver toxicity is usually not dose limiting, and the risk depends on the chemical and physical characteristics of the molecule and its clearance pathways.

7.3 Brachytherapy

Brachytherapy (percutaneous or at laparotomy) is a less common strategy to deliver radiation to liver cancers (Thomas et al. 1993; Donath et al. 1990; Ricke et al. 2004). Brachytherapy with applicators placed at laparotomy has not been associated with liver toxicity. Serious toxicity has been reported following percutaneous brachytherapy. In a phase II study of percutaneous Iridium-192 in 20 patients with liver cancer (19 metastases, 1 cholangiocarcinoma; mean diameter 7.7 cm (5.5–10.8 cm) for peripheral lesions and 3.6 cm (2.2–4.9 cm) for hilar cancers; dose range 12–25 Gy), two serious complications were observed. An intrahepatic hemorrrhage on removal of the brachytherapy sources was seen, and obstructive jaundice occurred 14 days after brachytherapy with elevated bilirubin and subsequent liver failure 9 months later, perhaps associated with biliary injury from high dose radiation. Mild increases in liver enzymes and bilirubin without clinical symptoms were common. (Ricke et al. 2004).

7.4 Biliary and Gallbladder Tolerance

Bile duct epithelium is relatively resistant to radiation injury. Biliary toxicity includes acute edema induced biliary obstruction (following irradiation of pending obstructing lesions) and late biliary strictures. Biliary toxicity has not been commonly reported following conventional fractionated external beam radiation therapy or SBRT, but has been described following intraductal brachytherapy.

Rabbit and dog animal models have revealed that single radiation doses above 30 Gy caused biliary duct stenosis which may lead to biliary cirrhosis over time (Todoroki 1978; Sindelar et al. 1982).

Biliary strictures have been seen years following hypofractionated proton therapy for hepatocellular carcinoma (Chiba et al. 2005). Totally, 3 of 162 patients treated with hypofractionated proton therapy developed biliary stenosis, or biomas 13, 29, and 38 months following therapy. This was most common with the fractionation schemes that used more than 4 Gy per fraction (72 Gy in 16 fractions and 50 Gy in 10 fractions).

The possibility for acute biliary obstruction following SBRT was reported in patients with cholangiocarcinoma treated with 5 Gy fractions or more, likely due to treatment-induced edema (Tse et al. 2008), suggesting that lower fraction sizes and/or prefraction steroids to reduce edema could reduce the possibility for treatment-induced edema and biliary obstruction or cholangitis.

There is little known about the gallbladder tolerance to radiation therapy. In theory, stricture of the cystic duct may result in edema or perforation of the gall bladder, so very high doses and high doses per fraction should be used with caution in this region. It is not known what the tolerance of the gallbladder wall is to irradiation.

Longer follow-up of patients treated with SBRT is required before the biliary tolerance for stricture and gallbladder tolerance to different doses per fraction is better understood.

8 Prevention and Management

8.1 Prevention

Animal models have investigated various interventions to mitigate and prevent classic and nonclassic RILD. No radioprotective effect of the highest tolerable doses of salicylates were found in rat models (Kinzie et al. 1972). Anticoagulation with warfarin have been suggested to be a potential mitigating treatment for classic RILD (Lightdale et al. 1979), but this has not been compared in a prospective setting, and there are risk of anticoagulation therapy in patients with liver disease, who are often those who require irradiation.

Several analyses in BMT patients have demonstrated less frequent symptoms and lower incidences of VOD in patients receiving heparin, defibrotide, and/or prostaglandin E1 (Chalandon et al. 2004; Rosenthal et al. 1996; Simon et al. 2001), suggesting a possible mitigating role of these agents for VOD liver toxicity. Randomized trials of these therapies in high-risk patients are warranted.

8.2 Management

Once any radiation therapy induced liver toxicity has been detected, a referral to a hepatologist is recommended. As in chronic liver disease, fluid and salt restriction, along with other conservative measures may delay the progression to liver failure.

No established standard exists for the treatment of RILD. Management is typically conservative, and limited to

supportive care with diuretics, paracentesis, and steroids. Classic reports have described the natural course of RILD as self-limited, with most patients' symptoms resolving over several months (Lawrence et al. 1995). The patients who do not respond to supportive management may develop chronic liver fibrosis, marked by portal hypertension, jaundice, ascites, coagulopathy, and general liver failure. Mortality rates from RILD range from 10 to 20 %, to 76 % (in patients with chronic viral hepatitis and/or liver cirrhosis), emphasizing the importance of preserving the liver function after radiation therapy when possible.

8.2.1 Supportive Therapy

Many noncytotoxic drugs administered concurrently with chemotherapy can cause abnormal liver function and should be considered potentially causative in the setting of abnormal liver function tests occurring during treatment. Allopurinol, commonly given with chemotherapy to prevent uric acid nephropathy and secondary gout, has been linked to fulminant hepatic failure, presumably due to a hypersensitivity reaction. Several antibiotics and antifungal agents can cause significant hepatic injury. While penicillins have a record of low hepatotoxicity, raised transaminases, and cholestatic jaundice have been reported with the commonly used antibiotic piperacillin-tazobactam, the potential of erythromycin and several other macrolides to cause (usually cholestatic) hepatitis is well established and fluconazole can cause hepatitis and can produce abnormal liver enzymes without significant liver biopsy changes. The 5HT3 receptor antagonists, ondansetron, and granisetron are associated with transient, reversible increases in transaminases and cholestatic jaundice and biliary stasis can occur with prochlorperazine, particularly during the first few months of treatment. With the current popularity of alternative medicines the occurrence of hepatotoxicity has led to the recognition of "herbal hepatitis". Up to 50 % of patients with cancer might not tell their doctor about use of alternative medications so a careful history is important.

9 Future Research

There are still many unanswered questions about radiation-induced liver toxicity, and research to better understand the pathophysiology of classic and nonclassic RILD are warranted. No intervention currently has been proven in patients to prevent or reverse the effects of RILD. By examining the mechanisms behind the pathogenesis of RILD, key areas of investigation to develop potential mitigating and preventative therapies may be identified. Some areas of active research include hepatocyte and stem cell rescue of liver injury, and development of antistellate cell and anti-TGF-β therapies.

The impact of concurrent or sequential systemic treatment on the radiation tolerance of the liver needs to be better defined, as there is a rationale to combine radiation therapy with systemic therapy in many clinical situations.

Improvements in the understanding of the partial liver tolerance to the liver may occur with collaborative efforts, and pooling of dose–volume information, clinical factors, and measurements of liver function pre- and post-radiation therapy is suggested. With such efforts, we may have more power to better understand how different dose distributions, and fractionations alter the tolerance of the liver to radiation therapy. Knowledge of the dose thresholds for subregional injury and of the doses associated with preservation of liver function and liver hypertrophy following therapy should help future NTCP modeling of injury and prevention of injury. Improved measured of liver function, and of the spatial differences in liver function, i.e., with novel imaging, would allow radiation plans to be developed to better avoid the best functioning portions of the liver, and possibly reduce the risk of hepatic toxicities. Finally, more research and clinical data on potential hepatobiliary toxicities that may occur following very high dose per fraction, i.e., SBRT, are also needed.

10 Review of Literature Landmarks (History and Literature Landmarks)

In 1954, Phillips et al. described one of the first cases of possible liver toxicity that occurred in one of 36 patients with liver metastases who were treated with estimated whole liver doses of 20–37 Gy in 8 fractions (Phillips et al. 1954). Subsequent reports of liver toxicity in the 1960s confirmed the low tolerance of the whole liver to irradiation (Ogata et al. 1963; Ingold et al. 1965; Schacter et al. 1986). In 1965, Ingold et al. described liver toxicity in 13 of 40 patients irradiated for abdominal diseases. Symptoms of rapid weight fain, increased abdominal girth, hepatomegaly were seen within 3 months following irradiation (Ingold et al. 1965). The liver enzymes, particularly the alkaline phosphatase, were elevated. Most of the patients recovered but a few died of liver failure. In 1966, Reed and Cox described the pathology in these cases, establishing features of classic radiation-induced liver disease (RILD) (Reed and Cox 1966). The early estimations of the whole liver tolerance to irradiation, 30–35 Gy with conventional fractionation, have remained largely unchanged.

Although Ingold reported that 55 Gy could be delivered safely to a portion of the liver in 1965, it was not until decades later that the partial liver tolerance to irradiation was quantified. With CT-based radiation therapy planning and clinical experience in partial liver irradiation, the relationship between radiation dose, liver volume irradiated,

and risk of liver toxicity has been described using mathematical models in various populations (Cheng et al. 2003; Liang et al. 2006; Dawson et al. 2001, 2002; Chiba et al. 2005; Jackson et al. 1995). These models show that the risk of toxicity increases as the irradiated liver volume, the dose, and the dose per fraction increase, at least for some of the liver toxicity endpoints (e.g. classic RILD). Clinical factors associated with increased risk of toxicity include tumor type (primary liver cancer versus metastases), type of chemotherapy used, and presence of hepatitis B virus (Cheng et al. 2004a). For classic RILD, the mean liver dose is a good estimate of toxicity risk, with 5 and 50 % risks of toxicity occurring with mean liver doses of 32 and 40 Gy, in 1.5 Gy twice daily, for patients with primary liver cancer, with a Child-Pugh score of A. Similar mean liver doses associated with 5 and 50 % risk levels for patients with metastases (without underlying liver disease) are 37 and 47 Gy, in 1.5 Gy twice daily. Reduced tolerance doses have been reported in Asian populations with hepatocellular carcinoma, where the incidence of Hepatitis B or C and cirrhosis is very high.

Bone marrow transplant and hematopoietic stem cell transplant, with and without TBI, has also been associated with liver toxicity, which is similar in clinical presentation to RILD, with the primary exception that RILD is anicteric, whereas transplant and TBI associated liver toxicity presents with an elevation in bilirubin.

Liver directed radioisotope therapy has been used to treat primary and metastatic liver cancers, and these therapies are also associated with a risk of liver toxicity. Although the risk of liver toxicity appears low in appropriately selected patients, both classic and nonclassic RILD can be seen following radioisotope therapy.

Acknowledgments Thanks to Dr Mark Lee and Dr. Catherine Coolens for their thoughtful comments on this chapter.

References

Abrams RA, Cardinale RM, Enger C et al (1997) Influence of prognostic groupings and treatment results in the management of unresectable hepatoma: experience with Cisplatinum-based chemoradiotherapy in 76 patients. Int J Radiat Oncol Biol Phys 39:1077–1085

Alati T, Van Cleeff M, Strom SC et al (1988) Radiation sensitivity of adult human parenchymal hepatocytes. Radiat Res 115:152–160

Alati T, Van Cleeff M, Jirtle RL (1989a) Radiosensitivity of parenchymal hepatocytes as a function of oxygen concentration. Radiat Res 118:488–501

Alati T, Eckl P, Jirtle RL (1989b) An in vitro micronucleus assay for determining the radiosensitivity of hepatocytes. Radiat Res 119:562–568

Amento EP, Beck LS (1991) TGF-beta and wound healing. Ciba Found Symp 157:115–123 discussion 123–129

Anscher MS, Crocker IR, Jirtle RL (1990) Transforming growth factor-beta 1 expression in irradiated liver. Radiat Res 122:77–85

Anscher MS, Peters WP, Reisenbichler H et al (1993a) Transforming growth factor beta as a predictor of liver and lung fibrosis after autologous bone marrow transplantation for advanced breast cancer. N Engl J Med 328:1592–1598

Anscher MS, Peters WP, Reisenbichler H, Petros WP, Jirtle RL (1993b) N Engl J Med 328:1592–1598

Austin-Seymour MM, Chen GT, Castro JR et al (1986) Dose volume histogram analysis of liver radiation tolerance. Int J Radiat Oncol Biol Phys 12:31–35

Bader TR, Herneth AM, Blaicher W et al (1998) Hepatic perfusion after liver transplantation: noninvasive measurement with dynamic single-section CT. Radiology 209:129–134

Barcellos-Hoff MH (2005a) How tissues respond to damage at the cellular level: orchestration by transforming growth factor-{beta} (TGF-{beta}). BJR Suppl 27:123–127

Barcellos-Hoff MH (2005b) Integrative radiation carcinogenesis: interactions between cell and tissue responses to DNA damage. Semin Cancer Biol 15:138–148

Barcellos-Hoff MH, Park C, Wright EG (2005) Radiation and the microenvironment—tumorigenesis and therapy. Nat Rev Cancer 5:867–875

Bearman SI (2001) Avoiding hepatic veno-occlusive disease: what do we know and where are we going? Bone Marrow Transplant 27:1113–1120

Bearman SI, Anderson GL, Mori M et al (1993) Venoocclusive disease of the liver: development of a model for predicting fatal outcome after marrow transplantation. J Clin Oncol 11:1729–1736

Beetz A, Messer G, Oppel T et al (1997) Induction of interleukin 6 by ionizing radiation in a human epithelial cell line: control by corticosteroids. Int J Radiat Biol 72:33–43

Bjornsson E (2006) Drug-induced liver injury: Hy's rule revisited. Clin Pharmacol Ther 79:521–528

Blobe GC, Schiemann WP, Lodish HF (2000) Role of transforming growth factor beta in human disease. N Engl J Med 342:1350–1358

Blomgren H, Lax I, Naslund I et al (1995) Stereotactic high dose fraction radiation therapy of extracranial tumors using an accelerator. Clinical experience of the first thirty-one patients. Acta Oncol 34:861–870

Blomley MJ, Coulden R, Dawson P et al (1995) Liver perfusion studied with ultrafast CT. J Comput Assist Tomogr 19:424–433

Borgelt BB, Gelber R, Brady LW et al (1981) The palliation of hepatic metastases: results of the Radiation Therapy Oncology Group pilot study. Int J Radiat Oncol Biol Phys 7:587–591

Brooks SE, Miller CG, McKenzie K et al (1970) Acute veno-occlusive disease of the liver. Fine structure in Jamaican children. Arch Pathol 89:507–520

Bruno S, Maisonneuve P, Castellana P et al (2005) Incidence and risk factors for non-alcoholic steatohepatitis: prospective study of 5408 women enrolled in Italian tamoxifen chemoprevention trial. BMJ 330:932

Burman C, Kutcher GJ, Emami B et al (1991) Fitting of normal tissue tolerance data to an analytic function. Int J Radiat Oncol Biol Phys 21:123–135

Cao Y, Pan C, Balter JM et al (2008) Liver function after irradiation based on computed tomographic portal vein perfusion imaging. Int J Radiat Oncol Biol Phys 70:154–160

Carlini P, Papaldo P, Fabi A et al (2006) Liver toxicity after treatment with gefitinib and anastrozole: drug–drug interactions through cytochrome p450? J Clin Oncol 2006:60–61

Castilla A, Prieto J, Fausto N (1991) Transforming growth factors beta 1 and alpha in chronic liver disease. Effects of interferon alfa therapy. N Engl J Med 324:933–940

Chalandon Y, Roosnek E, Mermillod B et al (2004) Prevention of veno-occlusive disease with defibrotide after allogeneic stem cell transplantation. Biol Blood Marrow Transplant 10:347–354
Cheng JC, Wu JK, Huang CM et al (2002) Radiation-induced liver disease after radiotherapy for hepatocellular carcinoma: clinical manifestation and dosimetric description. Radiother Oncol 63:41–45
Cheng JC, Wu JK, Huang CM et al (2003) Dosimetric analysis and comparison of three-dimensional conformal radiotherapy and intensity-modulated radiation therapy for patients with hepatocellular carcinoma and radiation-induced liver disease. Int J Radiat Oncol Biol Phys 56:229–234
Cheng JC, Liu MC, Tsai SY et al (2004a) Unexpectedly frequent hepatitis B reactivation by chemoradiation in postgastrectomy patients. Cancer 101:2126–2133
Cheng JC, Liu HS, Wu JK et al (2005) Inclusion of biological factors in parallel-architecture normal-tissue complication probability model for radiation-induced liver disease. Int J Radiat Oncol Biol Phys 62:1150–1156
Chiba T, Tokuuye K, Matsuzaki Y et al (2005) Proton beam therapy for hepatocellular carcinoma: a retrospective review of 162 patients. Clin Cancer Res 11:3799–3805
Chou CH, Chen PJ, Lee PH et al (2007) Radiation-induced hepatitis B virus reactivation in liver mediated by the bystander effect from irradiated endothelial cells. Clin Cancer Res 13:851–857
Christiansen H, Sheikh N, Saile B et al (2007) X-irradiation in rat liver: consequent upregulation of hepcidin and downregulation of hemojuvelin and ferroportin-1 gene expression. Radiology 242:189–197
Coeman DC, Verbeken EK, Nackaerts KL et al (2000) A fatal case of cholestatic liver failure probably related to gemcitabine. Ann Oncol 11:1503
Concannon JP, Edelmann A, Frich JC Jr et al (1967) Localized "radiation hepatitis" as demonstrated by scintillation scanning. Radiology 89:136–139
Couinaud C (1992) Anatomie du foie. Ann Ital Chir 63:693–697
Couvelard A, Scoazec JY, Dauge MC et al (1996) Structural and functional differentiation of sinusoidal endothelial cells during liver organogenesis in humans. Blood 87:4568–4580
Davila M, Bresalier R (2008) Gastrointestinal complications of oncologic therapy. Nat Clin Pract Gastroenterol Hepatol 5:682–696
Dawson LA, Ten Haken RK (2005) Partial volume tolerance of the liver to radiation. Semin Radiat Oncol 15:279–283
Dawson LA, Brock KK, Kazanjian S et al (2001) The reproducibility of organ position using active breathing control (ABC) during liver radiotherapy. Int J Radiat Oncol Biol Phys 51:1410–1421
Dawson LA, Eccles C, Bissonnette JP et al (2005a) Accuracy of daily image guidance for hypofractionated liver radiotherapy with active breathing control. Int J Radiat Oncol Biol Phys 62:1247–1252
DeLeve LD (1994) Dacarbazine toxicity in murine liver cells: a model of hepatic endothelial injury and glutathione defense. J Pharmacol Exp Ther 268:1261–1270
DeLeve LD (1996) Cellular target of cyclophosphamide toxicity in the murine liver: role of glutathione and site of metabolic activation. Hepatology 24:830–837
DeLeve LD (1998) Glutathione defense in non-parenchymal cells. Semin Liver Dis 18:403–413
DeLeve LD (2007) Hepatic microvasculature in liver injury. Semin Liver Dis 27:390–400
DeLeve LD, McCuskey RS, Wang X et al (1999) Characterization of a reproducible rat model of hepatic veno-occlusive disease. Hepatology 29:1779–1791
DeLeve LD, Shulman HM, McDonald GB (2002) Toxic injury to hepatic sinusoids: sinusoidal obstruction syndrome (veno-occlusive disease). Semin Liver Dis 22:27–42
DeLeve LD, Wang X, Tsai J et al (2003) Sinusoidal obstruction syndrome (veno-occlusive disease) in the rat is prevented by matrix metalloproteinase inhibition. Gastroenterology 125:882–890
Donath D, Nori D, Turnbull A et al (1990) Brachytherapy in the treatment of solitary colrectal metastases to the liver. J Surg Oncol 44:55–61
Emami B, Lyman J, Brown A et al (1991) Tolerance of normal tissue to therapeutic irradiation. Int J Radiat Oncol Biol Phys 21:109–122
Fajardo LF, Colby TV (1980) Pathogenesis of veno-occlusive liver disease after radiation. Arch Pathol Lab Med 104:584–588
Fedorocko P, Egyed A, Vacek A (2002) Irradiation induces increased production of haemopoietic and proinflammatory cytokines in the mouse lung. Int J Radiat Biol 78:305–313
Ganem G, Saint-Marc GMF, Kuentz M et al (1988) Venocclusive disease of the liver after allogeneic bone marrow transplantation in man. Int J Radiat Oncol Biol Phys 14:879–884
Geraci JP, Mariano MS, Jackson KL (1991) Hepatic radiation injury in the rat. Radiat Res 125:65–72
Goin JE, Salem R, Carr BI et al (2005a) Treatment of unresectable hepatocellular carcinoma with intrahepatic yttrium 90 microspheres: a risk-stratification analysis. J Vasc Interv Radiol 16:195–203
Goin JE, Salem R, Carr BI et al (2005b) Treatment of unresectable hepatocellular carcinoma with intrahepatic yttrium 90 microspheres: factors associated with liver toxicities. J Vasc Interv Radiol 16:205–213
Gourmelon P, Marquette C, Agay D et al (2005) Involvement of the central nervous system in radiation-induced multi-organ dysfunction and/or failure. BJR Suppl 27:62–68
Gray B, Hazel GV, Hope M et al (2001) Randomised trial of SIR-Spheres plus chemotherapy versus chemotherapy alone for treating patients with liver metastases from primary large bowel cancer. Ann Oncol 12:1711–1720
Gushiken F (2000) Peliosis hepatis after treatment with 2-chloro-3′-deoxyadenosine. South Med J 93:625–626
Haddad E, LeBourgeois J, Kuentz M et al (1983) Liver complications in lymphomas treated with a combination of chemotherapy and radiotherapy: preliminary results. Int J Radiat Oncol Biol Phys 9:1313–1319
Hata M, Tokuuye K, Sugahara S et al (2006) Proton beam therapy for hepatocellular carcinoma with limited treatment options. Cancer 107:591–598
Herfarth KK, Debus J, Lohr F et al (2001) Stereotactic single-dose radiation therapy of liver tumors: results of a phase I/II trial. J Clin Oncol 19:164–170
Herfarth KK, Hof H, Bahner ML et al (2003) Assessment of focal liver reaction by multiphasic CT after stereotactic single-dose radiotherapy of liver tumors. Int J Radiat Oncol Biol Phys 57:444–451
Herfarth KK, Debus J, Wannenmacher M (2004) Stereotactic radiation therapy of liver metastases: update of the initial phase-I/II trial. Front Radiat Ther Oncol 38:100–105
Ho C, Davis J, Anderson F et al (2005) Side effects related to cancer treatment: case 1 Hepatitis following treatment with gefitinib. J Clin Oncol 23:8531–8533
Hoefs JC, Chen PT, Lizotte P (2006) Noninvasive evaluation of liver disease severity. Clin Liver Dis 10:535–562, viii–ix
Hosoi Y, Miyachi H, Matsumoto Y et al (2001) Induction of interleukin-1beta and interleukin-6 mRNA by low doses of ionizing radiation in macrophages. Int J Cancer 96:270–276

Hoyer M, Roed H, Traberg Hansen A et al (2006) Phase II study on stereotactic body radiotherapy of colorectal metastases. Acta Oncol 45:823–830

Iguchi T, Sato S, Kouno Y et al (2003) Comparison of Tc-99m-GSA scintigraphy with hepatic fibrosis and regeneration in patients with hepatectomy. Ann Nucl Med 17:227–233

Ingold J, Reed G, Kaplan H (1965) Radiation hepatitis. Am J Roentgenol 93:200–208

Ishihara H, Tsuneoka K, Dimchev AB et al (1993) Induction of the expression of the interleukin-1 beta gene in mouse spleen by ionizing radiation. Radiat Res 133:321–326

Jackson A, Ten Haken RK, Robertson JM et al (1995) Analysis of clinical complication data for radiation hepatitis using a parallel architecture model. Int J Radiat Oncol Biol Phys 31:883–891

Jeffrey RB Jr, Moss AA, Quivey JM et al (1980) CT of radiation-induced hepatic injury. AJR Am J Roentgenol 135:445–448

Jirtle RL, Michalopoulos G, McLain JR et al (1981) Transplantation system for determining the clonogenic survival of parenchymal hepatocytes exposed to ionizing radiation. Cancer Res 41:3512–3518

Jirtle RL, McLain JR, Strom SC et al (1982) Repair of radiation damage in noncycling parenchymal hepatocytes. Br J Radiol 55:847–851

Jirtle RL, Michalopoulos G, Strom SC et al (1984) The survival of parenchymal hepatocytes irradiated with low and high LET radiation. Br J Cancer Suppl 6:197–201

Jirtle R, Anscher M, Alati T (1990) Radiation sensitivity of the liver. Adv Radiat Biol 14:269–311

Jungermann K (1988) Metabolic zonation of liver parenchyma. Semin Liver Dis 8:329–341

Kavanagh BD, Schefter TE, Cardenes HR et al (2006) Interim analysis of a prospective phase I/II trial of SBRT for liver metastases. Acta Oncol 45:848–855

Kawashima M, Furuse J, Nishio T et al (2005) Phase II study of radiotherapy employing proton beam for hepatocellular carcinoma. J Clin Oncol 23:1839–1846

Kennedy AS, Nutting C, Coldwell D et al (2004) Pathologic response and microdosimetry of (90)Y microspheres in man: review of four explanted whole livers. Int J Radiat Oncol Biol Phys 60:1552–1563

Kennedy AS, Coldwell D, Nutting C et al (2006) Resin 90Y-microsphere brachytherapy for unresectable colorectal liver metastases: modern USA experience. Int J Radiat Oncol Biol Phys 65:412–425

Khalil N (1999) TGF-beta: from latent to active. Microbes Infect 1:1255–1263

Kim TH, Kim DY, Park JW et al (2007) Dose-volumetric parameters predicting radiation-induced hepatic toxicity in unresectable hepatocellular carcinoma patients treated with three-dimensional conformal radiotherapy. Int J Radiat Oncol Biol Phys 67:225–231

King PD, Perry MC (2001) Hepatotoxicity of chemotherapy. Oncologist 6:162–176

Kinzie J, Studer RK, Perez B et al (1972) Noncytokinetic radiation injury: anticoagulants as radioprotective agents in experimental radiation hepatitis. Science 175:1481–1483

Klinger M, Eipeldauer S, Hacker S et al (2009) Bevacizumab protects against sinusoidal obstruction syndrome and does not increase response rate in neoadjuvant XELOX/FOLFOX therapy of colorectal cancer liver metastases. Eur J Surg Oncol 35:515–520

Kopetz S, Vauthey JN (2008) Perioperative chemotherapy for resectable hepatic metastases. Lancet 371:963–965

Lawrence TS, Ten Haken RK, Kessler ML et al (1992) The use of 3-D dose volume analysis to predict radiation hepatitis. Int J Radiat Oncol Biol Phys 23:781–788

Lawrence TS, Robertson JM, Anscher MS et al (1995) Hepatic toxicity resulting from cancer treatment [Review] [64 refs]. Int J Radiat Oncol Biol Phys 31:1237–1248

Ley K (1996) Molecular mechanisms of leukocyte recruitment in the inflammatory process. Cardiovasc Res 32:733–742

Lightdale CJ, Wasser J, Coleman M et al (1979) Anticoagulation and high dose liver radiation: a preliminary report. Cancer 43:174–181

Linard C, Ropenga A, Vozenin-Brotons MC et al (2003) Abdominal irradiation increases inflammatory cytokine expression and activates NF-kappaB in rat ileal muscularis layer. Am J Physiol Gastrointest Liver Physiol 285:G556–G565

Llovet JM, Ricci S, Mazzaferro V et al (2008) Sorafenib in advanced hepatocellular carcinoma. N Engl J Med 359:378–390

Lyman JT (1985) Complication probability as assessed from dose-volume histograms. Radiat Res Suppl 8:S13–S19

Materne R, Van Beers BE, Smith AM et al (2000) Non-invasive quantification of liver perfusion with dynamic computed tomography and a dual-input one-compartmental model. Clin Sci (Lond) 99:517–525

Meeren AV, Bertho JM, Vandamme M et al (1997) Ionizing radiation enhances IL-6 and IL-8 production by human endothelial cells. Mediators Inflamm 6:185–193

Mehendale HM (2005) Tissue repair: an important determinant of final outcome of toxicant-induced injury. Toxicol Pathol 33:41–51

Mendez RA, Wunderink W, Hussain SM et al (2006) Stereotactic body radiation therapy for primary and metastatic liver tumors: a single institution phase i–ii study. Acta Oncol 45:831–837

Miles KA (1991) Measurement of tissue perfusion by dynamic computed tomography. Br J Radiol 64:409–412

Miles KA, Hayball M, Dixon AK (1991) Colour perfusion imaging: a new application of computed tomography. Lancet 337:643–645

Miles KA, Hayball MP, Dixon AK (1993) Functional images of hepatic perfusion obtained with dynamic CT. Radiology 188:405–411

Moriconi F, Christiansen H, Raddatz D et al (2008) Effect of radiation on gene expression of rat liver chemokines: in vivo and in vitro studies. Radiat Res 169:162–169

Neff R, Abdel-Misih R, Khatri J et al (2008) The toxicity of liver directed yttrium-90 microspheres in primary and metastatic liver tumors. Cancer Invest 26:173–177

Ogata K, Hizawa K, Yoshida M et al (1963) Hepatic injury following irradiation–a morphologic study. Tokushima J Exp Med 43:240–251

Ogawa Y, Murata Y, Nishioka A et al (1998) Tamoxifen-induced fatty liver in patients with breast cancer. Lancet 351:725

Ohara K, Okumura T, Tsuji H et al (1997) Radiation tolerance of cirrhotic livers in relation to the preserved functional capacity: analysis of patients with hepatocellular carcinoma treated by focused proton beam radiotherapy. Int J Radiat Oncol Biol Phys 38:367–372

Order S, Donaldson S (2003) Hemangiomas, radiation therapy of benign diseases—a clinical guide, 2nd edn. Springer, Berlin, pp 133–134

Ostapowicz G, Fontana RJ, Schiodt FV et al (2002) Results of a prospective study of acute liver failure at 17 tertiary care centers in the United States. Ann Intern Med 137:947–954

Park HC, Seong J, Han KH et al (2002) Dose-response relationship in local radiotherapy for hepatocellular carcinoma. Int J Radiat Oncol Biol Phys 54:150–155

Pawlik TM, Olino K, Gleisner AL et al (2007) Preoperative chemotherapy for colorectal liver metastases: impact on hepatic histology and postoperative outcome. J Gastrointest Surg 11:860–868

Perez C, Korba A, Zivnuska F et al (1978) 60Co moving strip technique in the management of the ovary: analysis of tumor control and morbidity. Int J Radiat Oncol Biol Phys 4:279–388

Peters AM, Brown J, Hartnell GG et al (1987a) Non-invasive measurement of renal blood flow with 99mTc DTPA: comparison with radiolabelled microspheres. Cardiovasc Res 21:830–834
Peters AM, Gunasekera RD, Lavender JP et al (1987b) Noninvasive measurement of renal blood flow using DTPA. Contrib Nephrol 56:26–30
Phillips R, Karnofsku D, Hamilton L et al (1954) Roentgen therapy of hepatic metastases. Am J Roengenol 71:826
Rahmouni A, Montazel JL, Golli M et al (1992) Unusual complication of liver irradiation: acute thrombosis of a main hepatic vein: CT and MR imaging features. Radiat Med 10:163–166
Ramadori G, Armbrust T (2001) Cytokines in the liver. Eur J Gastroenterol Hepatol 13:777–784
Rappaport AM (1976) The microcirculatory acinar concept of normal and pathological hepatic structure. Beitrage zur Pathologie 157:215–243
Reiss U, Cowan M, McMillan A et al (2002) Hepatic venoocclusive disease in blood and bone marrow transplantation in children and young adults: incidence, risk factors, and outcome in a cohort of 241 patients. J Pediatr Hematol Oncol 24:746–750
Ricke J, Wust P, Stohlmann A et al (2004) CT-guided interstitial brachytherapy of liver malignancies alone or in combination with thermal ablation: phase I-II results of a novel technique. Int J Radiat Oncol Biol Phys 58:1496–1505
Robinson K, Lambiase L, Li J et al (2003) Fatal cholestatic liver failure associated with gemcitabine therapy. Dig Dis Sci 48:1804–1808
Rodriguez-Frias EA, Lee WM (2007) Cancer chemotherapy II: atypical hepatic injuries. Clin Liver Dis 11:663–676, viii
Rollins BJ (1986) Hepatic veno-occlusive disease. Am J Med 81:297–306
Rosenthal J, Sender L, Secola R et al (1996) Phase II trial of heparin prophylaxis for veno-occlusive disease of the liver in children undergoing bone marrow transplantation. Bone Marrow Transplant 18:185–191
Rubin P, Levitt SH (1964) The response of disseminated reticulum cell sarcoma to the intravenous injection of colloidal radioactive gold. J Nucl Med Off Publ Soc Nucl Med 5:581–594
Russell AH, Clyde C, Wasserman TH et al (1993) Accelerated hyperfractionated hepatic irradiation in the management of patients with liver metastases: results of the RTOG dose escalating protocol. Int J Radiat Oncol Biol Phys 27:117–123
Saif MW (2008) Hepatic failure and hepatorenal syndrome secondary to erlotinib. Safety reminder. J Pancreas 9:748–752
Sartori MT, Spiezia L, Cesaro S et al (2005) Role of fibrinolytic and clotting parameters in the diagnosis of liver veno-occlusive disease after hematopoietic stem cell transplantation in a pediatric population. Thromb Haemost 93:682–689
Schacter L, Crum E, Spitzer T et al (1986) Fatal radiation hepatitis: a case report and review of the literature. Gynecol Oncol 24:373–380
Schefter TE, Kavanagh BD, Timmerman RD et al (2005) A phase I trial of stereotactic body radiation therapy (SBRT) for liver metastases. Int J Radiat Oncol Biol Phys 62:1371–1378
Sempoux C, Horsmans Y, Geubel A et al (1997) Severe radiation-induced liver disease following localized radiation therapy for biliopancreatic carcinoma: activation of hepatic stellate cells as an early event. Hepatology 26:128–134
Seong J, Park HC, Han KH et al (2003) Clinical results and prognostic factors in radiotherapy for unresectable hepatocellular carcinoma: a retrospective study of 158 patients. Int J Radiat Oncol Biol Phys 55:329–336
Seong J, Shim SJ, Lee IJ et al (2007) Evaluation of the prognostic value of Okuda, cancer of the liver Italian program, and Japan integrated staging systems for hepatocellular carcinoma patients undergoing radiotherapy. Int J Radiat Oncol Biol Phys 67:1037–1042
Sessa C, Aamdal S, Wolff I et al (1994) Gemcitabine in patients with advanced malignant melanoma or gastric cancer: phase II studies of the EORTC Early Clinical Trials Group. Ann Oncol 5:471–472
Shulman HM, McDonald GB, Matthews D et al (1980) An analysis of hepatic venocclusive disease and centrilobular hepatic degeneration following bone marrow transplantation. Gastroenterology 79:1178–1191
Shulman HM, Gown AM, Nugent DJ (1987) Hepatic veno-occlusive disease after bone marrow transplantation. Immunohistochemical identification of the material within occluded central venules. Am J Pathol 127:549–558
Shulman HM, Fisher LB, Schoch HG et al (1994) Veno-occlusive disease of the liver after marrow transplantation: histological correlates of clinical signs and symptoms. Hepatology 19:1171–1181
Simon M, Hahn T, Ford LA et al (2001) Retrospective multivariate analysis of hepatic veno-occlusive disease after blood or marrow transplantation: possible beneficial use of low molecular weight heparin. Bone Marrow Transplant 27:627–633
Sindelar WF, Tepper J, Travis EL (1982) Tolerance of bile duct to intraoperative irradiation. Surgery 92:533–540
Speeg KV, Bay MK (1995) Prevention and treatment of drug-induced liver disease. Gastroenterol Clin North Am 24:1047–1064
Stubbs RS, Cannan RJ, Mitchell AW (2001) Selective internal radiation therapy (SIRT) with 90Yttrium microspheres for extensive colorectal liver metastases. Hepatogastroenterology 48:333–337
Tabbara IA, Zimmerman K, Morgan C et al (2002) Allogeneic hematopoietic stem cell transplantation: complications and results. Arch Intern Med 162:1558–1566
Ten Haken RK, Martel MK, Kessler ML et al (1993) Use of Veff and iso-NTCP in the implementation of dose escalation protocols. Int J Radiat Oncol Biol Phys 27:689–695
Ten Haken RK, Lawrence TS, Dawson LA (2006) Prediction of radiation-induced liver disease by Lyman normal-tissue complication probability model in three-dimensional conformal radiation therapy for primary liver carcinoma: in regards to Xu et al. (Int J Radiat Oncol Biol Phys 65:189–195). Int J Radiat Oncol Biol Phys 66:1272; author reply 1272–1273, 2006
Thomas DS, Nauta RJ, Rodgers JE et al (1993) Intraoperative high-dose rate interstitial irradiation of hepatic metastases from colorectal carcinoma. Results of a phase I-II trial. Cancer 71:1977–1981
Tian JH, Xu BX, Zhang JM et al (1996) Ultrasound-guided internal radiotherapy using yttrium-90-glass microspheres for liver malignancies. J Nucl Med 37:958–963
Todoroki T (1978) The late effects of single massive iradiation with electrons of the liver hilum of rabbits. Jpn J Gastrioentereol Surg 11:169–177
Tsai SL, Chen PJ, Lai MY et al (1992) Acute exacerbations of chronic type B hepatitis are accompanied by increased T cell responses to hepatitis B core and e antigens. Implications for hepatitis B e antigen seroconversion. J Clin Invest 89:87–96
Tse RV, Hawkins M, Lockwood G et al (2008) Phase I study of individualized stereotactic body radiotherapy for hepatocellular carcinoma and intrahepatic cholangiocarcinoma. J Clin Oncol 26:657–664
Uematsu M, Shioda A, Suda A et al (2000) Intrafractional tumor position stability during computed tomography (CT)-guided frameless stereotactic radiation therapy for lung or liver cancers with a fusion of CT and linear accelerator (FOCAL) unit. Int J Radiat Oncol Biol Phys 48:443–448
Unger EC, Lee JK, Weyman PJ (1987) CT and MR imaging of radiation hepatitis. J Comput Assist Tomogr 11:264–268

Vauthey JN, Pawlik TM, Ribero D et al (2006) Chemotherapy regimen predicts steatohepatitis and an increase in 90-day mortality after surgery for hepatic colorectal metastases. J Clin Oncol 24:2065–2072

Welsh JS, Kennedy AS, Thomadsen B (2006) Selective internal radiation therapy (SIRT) for liver metastases secondary to colorectal adenocarcinoma. Int J Radiat Oncol Biol Phys 66:S62–S73

Welsh FK, Tilney HS, Tekkis PP et al (2007) Safe liver resection following chemotherapy for colorectal metastases is a matter of timing. Br J Cancer 96:1037–1042

Wharton JT, Delclos L, Gallager S et al (1973) Radiation hepatitis induced by abdominal irradiation with the cobalt 60 moving strip technique. Am J Roentgenol Radium Ther Nucl Med 117:73–80

Wu DH, Liu L, Chen LH (2004) Therapeutic effects and prognostic factors in three-dimensional conformal radiotherapy combined with transcatheter arterial chemoembolization for hepatocellular carcinoma. World J Gastroenterol 10:2184–2189

Xu ZY, Liang SX, Zhu J et al (2006) Prediction of radiation-induced liver disease by Lyman normal-tissue complication probability model in three-dimensional conformal radiation therapy for primary liver carcinoma. Int J Radiat Oncol Biol Phys 65:189–195

Yaes RJ, Kalend A (1988) Local stem cell depletion model for radiation myelitis. Int J Radiat Oncol Biol Phys 14:1247–1259

Yamada K, Izaki K, Sugimoto K et al (2003) Prospective trial of combined transcatheter arterial chemoembolization and three-dimensional conformal radiotherapy for portal vein tumor thrombus in patients with unresectable hepatocellular carcinoma. Int J Radiat Oncol Biol Phys 57:113–119

Yeo W, Chan PK, Zhong S et al (2000) Frequency of hepatitis B virus reactivation in cancer patients undergoing cytotoxic chemotherapy: a prospective study of 626 patients with identification of risk factors. J Med Virol 62:299–307

Zorzi D, Laurent A, Pawlik TM et al (2007) Chemotherapy-associated hepatotoxicity and surgery for colorectal liver metastases. Br J Surg 94:274–286

Recommended Reading

Cheng JC, Wu JK, Lee PC et al (2004b) Biologic susceptibility of hepatocellular carcinoma patients treated with radiotherapy to radiation-induced liver disease. Int J Radiat Oncol Biol Phys 60:1502–1509

Dawson LA, Normolle D, Balter JM et al (2002) Analysis of radiation-induced liver disease using the Lyman NTCP model. Int J Radiat Oncol Biol Phys 53:810–821

Dawson LA, Biersack M, Lockwood G et al (2005b) Use of principal component analysis to evaluate the partial organ tolerance of normal tissues to radiation. Int J Radiat Oncol Biol Phys 62:829–837

Liang SX, Zhu XD, Xu ZY et al (2006) Radiation-induced liver disease in three-dimensional conformal radiation therapy for primary liver carcinoma: the risk factors and hepatic radiation tolerance. Int J Radiat Oncol Biol Phys 65:426–434

Pan C, Kavanagh B, Dawson L et al (2008) Radiation-associated liver injury. Int J Radiat Oncol Biol Phys

Reed G, Cox A (1966) The human liver after radiation injury. A form of veno-occlusive disease. Am J Pathol 48:597–611